2014

The TLC Method for Modeling Creep Deformation and Rupture

David May
University of Central Florida

THE TLC METHOD FOR MODELING CREEP DEFORMATION AND RUPTURE

by

DAVID MAY

A thesis submitted in partial fulfillment of the requirements
for the Honors in the Major in Mechanical Engineering
in the College of Engineering and Computer Science
and in The Burnett Honors College
at the University of Central Florida
Orlando, Florida

Spring Term 2014

Thesis Chair: Dr. Ali P. Gordon

ABSTRACT

This thesis describes a novel new method, termed the Tangent-Line-Chord (TLC) method, that can be used to more efficiently model creep deformation dominated by the tertiary regime. Creep deformation is a widespread mechanical mode of failure found in high-stress and temperature mechanical systems. To accurately simulate creep and its effect on structures, researchers utilize finite element analysis (FEA). General purpose FEA packages require extensive amounts of time and computer resources to simulate creep softening in components because of the large deformation rates that continuously evolve. The goal of this research is to employ multi-regime creep models, such as the Kachanov-Rabotnov model, to determine a set of equations that will allow creep to be simulated using as few iterations as possible. The key outcome is the freeing up of computational resources and the saving of time. Because both the number of equations and the value of material constants within the model change depending on the approach used, programming software will be utilized to automate this analytical process. The materials being considered in this research are mainly generic Ni-based superalloys, as they exhibit creep responses that are dominated by secondary and tertiary creep.

ACKNOWLEDGMENTS

I would like to acknowledge Dr. Gordon for recruiting me into his research group when I was at the end of my freshman year. I have learned more about the engineering profession in the lab than in all of my classes combined. I would also like to acknowledge Charles Mansfield, a current member of the Mechanics of Materials Research Group (MOMRG), and Calvin Stewart, an alumni of MOMRG, for patiently teaching me how to program in MATLAB and ANSYS.

TABLE OF CONTENTS

LIST OF FIGURES

LIST OF TABLES

CHAPTER 1: INTRODUCTION

1.1 Motivation

Finite element analysis (FEA) software is being utilized more frequently in the engineering industry as the complexity of mechanical systems is better understood and the cost of conducting experiments increases. When a mechanical component is placed into a high-stress, high-temperature, and high-use environment, the interaction between the physical processes is challenging to determine. Simulations are important in the energy sector where estimation of rupture lives of componentssuch as transition pieces (Figure 1.1a) and turbine blades (Figure 1.1b) are vital for safety. Although these components are subjected to high stresses at high temperatures, they are expected to last for years.

(a) **(b)**

Figure 1.1: Industrial gas turbine (a) transition pieces (Courtesy Combined Cycle Journal) and (b) turbine blades (Courtesy Siemens)

These types of components are comprised of primary creep resistant materials such as Ni-base superalloys. As such, primary creep is generally negligible while the secondary and tertiary creep

regimes dominate the creep life. These types of creep lives are highly nonlinear, and engineers generally assess the expected life of the component through FEA and rupture models, such as the Larson Miller Parameter.

A primary mode of failure in components found in industrial gas turbines is creep. The cost of a 40 MW industrial gas turbines is, on average, nearly twenty-seven million dollars [1]. If creep is not adequately characterized, then a part that needed to be replaced could catastrophically fail, which is expensive to the company and detrimental to its customers. Catastrophic failures that result from creep occur when tertiary creep is active for too long. This can happen if the proprietary creep models do not accurately characterize the extreme nonlinearities that arise during near-rupture tertiary creep. Thus, it is also necessary to develop creep models that can capture the near-rupture tertiary behavior in an efficient manner.

The goal of this research is to develop a reduced-order constitutive creep model that will have the ability to accurately and quickly simulate extensive creep. Constitutive modeling constants, which are typically optimized through regression, are optimized to best fit data over the entire time range. Candidate creep models for this research are the Norton model and the Kachanov-Rabotnov damage model. The Norton model is the fastest model to simulate, but it produces the most overall error when primary and tertiary regimes are dominant. The Kachanov-Rabotnov model is a slower model with respect to solve time, but it produces more accurate results.

When dealing with long-term creep tests (i.e., 10000+ hours), it is seen that the amount of non-linear regression involved to determine material constants is very high and as such, it takes

numerous valuable hours for a computer to complete the analysis. Creep simulations are usually conducted and coupled with experience and rupture experiments, to determine part replacement. Part replacement is ideally carried out before tertiary creep sets in. This is because metals usually rupture not long after this stage of deformation is reached. Subsequently, it is suggested that, for design purposes, the analysis can be simplified using a reduced-order model, albeit with a slightly increased tolerance for error that is still within the scatter of experimental data, so that the time to tertiary creep can be quickly determined.

1.2 Overview of Thesis

The following chapter will cover all pertinent background information. Chapter 3 explains and derivesa reduced-order modeling approach as well as summarizes the available test data. A parametric analysis and the results will be shown in Chapter 4. Chapter 5 compares the proposed reduced-order model to secondary and tertiary creep models based on the amount of CPU time required. The conclusions will be discussed in Chapter 6, while Chapter 7 proposes future work that can be carried out to further improve the reduced-order model. All of this isproceeded by a list of references and an appendix where all source codes will be included.

CHAPTER 2: BACKGROUND

The following sections explore the analytical methods involved in creep deformation modeling and their limitations. Approaches to reduced-order plasticity and creep modeling are also described.

2.1 Creep Deformation

Engineering strain is defined as a relative displacement of particles within a material .Geometrically, axial strain is defined by

$$\varepsilon = \frac{L_f - L_0}{L_o} \tag{2.1}$$

where L_f is the final length and L_0 is the initial length. A material will experience strain as a stress is applied to it. Creep strain is the inelastic deformation that occurs as a material undergoes agenerally quasi-staticstress, usually at elevated temperatures (40% of the melting temperature) for most industrial-grade metals. Creep can also occur at room temperature for softer metals such as lead. The rate at which deformation occurs depends on the characteristic stress and temperature as well as specific material behavior and geometry.

There are three microstructural mechanisms associated with creep in metals: bulk diffusion creep, grain boundary diffusion creep, and dislocation creep. Bulk diffusion creep, or Nabarro-Herring creep, is driven by material diffusion through grains. Stress gradients form within the material as the load is applied, with higher stresses occurring within the grain at the edges that lie along the loading direction. As this process is evolving, atoms diffuse through the

grains to the high stress locations, causing the grains to elongate. As the grains elongate, the strain rate decreases until it reaches steady-state, where it will continue to slowly creep until the grains begin to crack, at which the strain rate exponentially increases until rupture. As eachgrain elongates within the material, deformation is observed [2]. Grain boundary diffusion, also called Coble creep, is similar to Nabarro-Herring creep except that the diffusion path is primarily through the grain boundaries instead of the grains themselves.

Dislocation creep, or climb creep, results from the movement of dislocations that are incurred as the material reacts to the applied stress. As the load permeates a material, particles within the crystal lattice begin to dislocate along the glide plane [3]. As these dislocations move, ionic bonds are broken. New bonds are then reformed between the newly adjacent particles, and as the dislocations accumulate, the bonds become stronger and more resistant to creep. Once a critical strain is reached, the stronger bonds begin to break and an exponential strain rate is observed.

Primary creep is characterized by a decreasing strain rate and is physically produced by dislocations and strain hardening within the material as the material is introduced to the load. Secondary creep is characterized by a near-constant strain rate that is considered a transitionary period between hardening (primary creep) and softening (tertiary creep). In this stage, the strength of the dislocations have reached a semi steady-state until they reach a critical strain, at which point tertiary creep sets in. Tertiary creep is considered the softening stage and is characterized by the formation of cracks along the grain boundaries within the material [4]. A complete creep curve is illustrated in Figure 2.1.

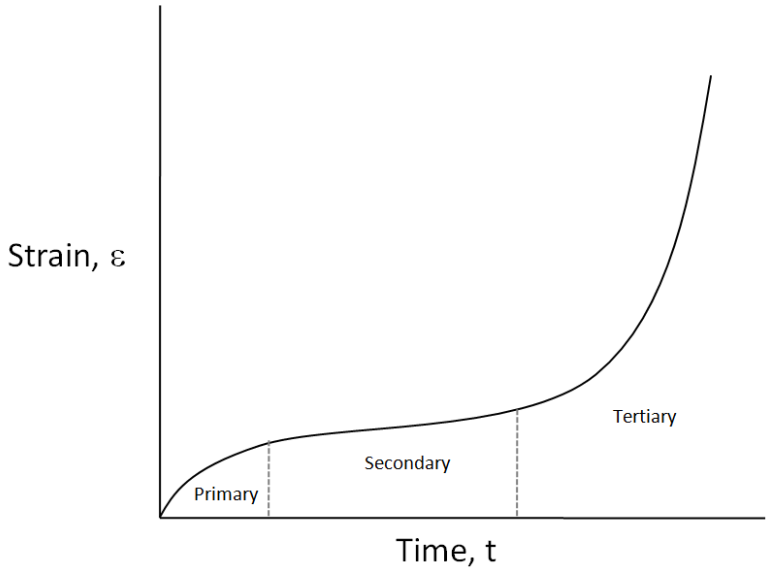

Figure 2.1: Creep curve showing individual creep regimes

Ni-based superalloys, which are commonly used in gas turbine components, will experience relatively short periods of quasi-static loading, during which creep will occur. When these conditions are held, critical locations of components will display secondary creep or tertiary creep. This is largely in part to the exceptional primary creep resistance of superalloys [5]. Extensive creep simulations become problematic with components that exhibit long tertiary creep lives because of the high degree of nonlinearity of tertiary creep. The nonlinearities arise because microscopic voids within the material accumulate, which results in a net area reduction that increases the effective stress and therefore strain rate. It is not uncommon to see strain rates reach 0.5 %/hr or even 1.0 %/hr.

2.2 Creep Models

Creep models are designed to correlate experimentally-acquired strain histories as a material experiences quasi-static stress. Accuracy is gauged based on how well it correlates to physical test data, including strains and strain rates. An example of a creep model accurately capturing primary and secondary creep behavior is shown in Figure 2.2.

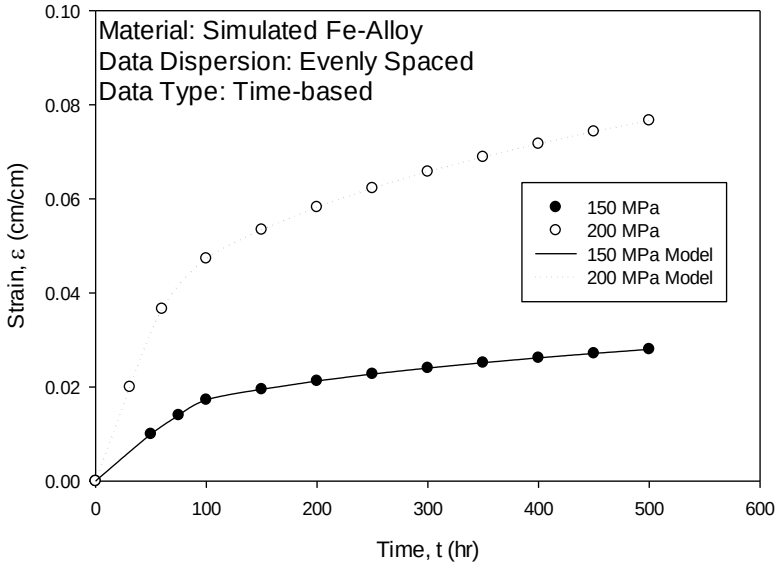

Figure 2.2: Primary and secondary creep modeling of a generic steel alloy [6]

Creep models can be given as creep, ε_{cr}, or creep rate, $\dot{\varepsilon}_{cr}$. In most instances, creep deformation formulae take the characteristic of

$$\dot{\varepsilon}_{cr} = f(\sigma)g(T)h(t) \tag{2.2}$$

where σ is stress, T is temperature, and t is time. To capture the behavior of the test material, unique constants are embedded into the mathematical models that are generally temperature-dependent; however, more complex creep models will contain both temperature and stress-dependent constants that can more accurately model creep on parts that experience stress and temperature gradients.

Some examples of common creep models are the Norton model [7], the Theta-Projection Model [8], and the Kachanov-Rabotnov model [9,10]. The Norton equation is given by

$$\dot{\varepsilon}_{cr} = A\sigma^n \tag{2.2}$$

where A and n are material constants, σ is stress in MPa, and t is time in hr[6]. This model captures the secondary creep regime well. It is a simple linear equation with a slope, $A\sigma^n$, multiplying the independent variable, t. The Norton model is usually modified with the Arrhenius equation to capture temperature-dependence. In other cases, a time-hardening exponent, m, is incorporated into the time variable so that primary creep can be modeled[4].

The Theta-Projection model, developed by Evans and Wilshire [8] is defined as

$$\varepsilon_{cr} = \theta_1\left(1-e^{-\theta_2 t}\right)+\theta_3\left(e^{\theta_4 t}-1\right) \tag{2.3}$$

where θ_1 through θ_4 are material constants and t is time in hr. This model correlations the full range of creep, but there are two main drawbacks. The four material constants, θ_1-θ_4, have no physical significance and are difficult to determine from experimental data alone. They are generally determined using extensive multi-variate regression routines. The second is that this

model inherently describes creep as a combination of creep softening and creep hardening, which correlates to a weakness of modeling long periods of secondary creep. The secondary creep regime is merely a small time period in which a decreasing creep rate transitions into an increasing creep rate [11].This is detrimental to this research because the materials being analyzed have creep lives that exhibit long periods of secondary and tertiary creep, with very little if any primary creep.

The Kachanov-Rabotnov model is given as

$$\dot{\varepsilon}_{cr} = A\left(\frac{\sigma}{1-\omega}\right)^{n} \tag{2.4}$$

where the damage evolution is defined as

$$\dot{\omega} = \frac{M\sigma^{\chi}}{(1-\omega)^{\phi}} \tag{2.5}$$

The variables A, n, M, χ, and ϕ are material constants. This model introduces the concept of damage, ω, which simulates the physical phenomenon such as voids that begin accumulating at early stages of creep and then evolve as micro cracks over the entire creep life [4,9,10]. This variable continually increases from zero to unity with the progression of creep, with a value of one representing rupture. The continuous evolution of damage within the creep rate and damage rate allows the Kachanov-Rabotnov model to capture the nonlinear characteristic of tertiary creep with more insight than the previously discussed models. An important characteristic of the Kachanov-Rabotnov formulation is the equation reduces to the Norton model if damage evolution is restricted.

2.3 Limitations of Tertiary Creep Models

Creep models that explicitly model tertiary creep have not been developed. Any creep models that can model tertiary creep are also required to model secondary creep because all creep data includes some form of secondary creep. To adequately characterize a near linear creep response and a highly nonlinear response simultaneously, there must either be individual terms that describe each creep regime, i.e. Theta-Projection model,or a differential term that can account for evolving changes in strain rate, i.e. Kachanov-Rabotnov model. In both cases, tertiary creep is modeled as a nonlinear response that can reach strain rates of more than 1 %/hr.

When strain rates reach this magnitude, the computational resources that are required to converge on a solution increase dramatically. At the onset of tertiary creep, damage starts to accumulate and the material begins to neck. Because of these two factors, the effective stress increases at an increasing rate, which translates into an increasing strain rate. Increasing strain rates cause the Newton-Raphson method to use an increasingly higher number of iterations to converge, and the solve time is directly proportional to the number of Newton-Raphson iterations. Figure 2.3 illustrates this relationship between number of iterations and strain rate.

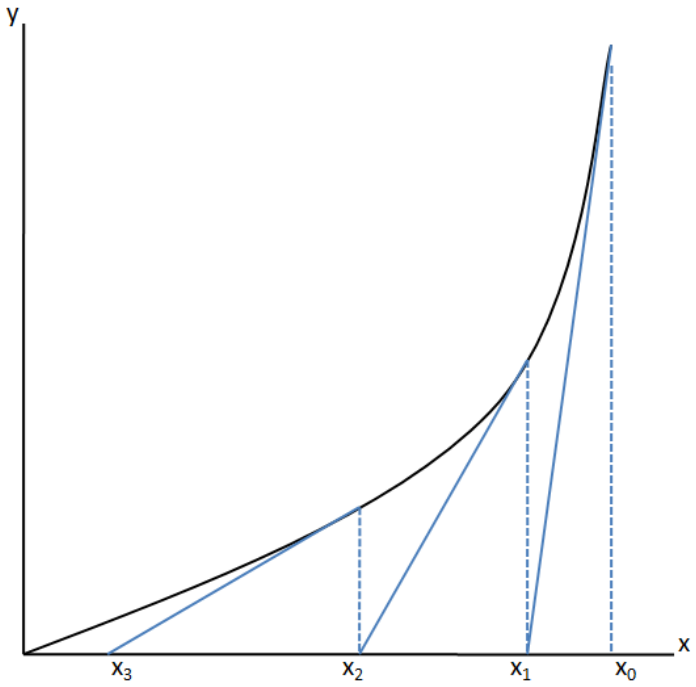

Figure 2.3: Illustration of newton-raphson method applied to increasing rates

In finite element simulations, a converged solution is determined for each time step, which means that the iterative process illustrated in Figure 2.3 is repeated numerous times. If no convergence is found within a set number of iterations, then the time step is decreased and the process is repeated until a solution is determined.

From Figure 2.1, it is observed that the near-rupture portion of tertiary creep is linear. The Newton-Raphson method can converge in one iteration for such linear responses. However, the constitutive models that are used to model tertiary creep represent creep with nonlinear mathematical relationships, and because the Newton-Raphson is an equation driven solver, it treats the seemingly linear response as nonlinear.

2.4 Reduced-Order Plasticity Models

Reduced-order models are commonly employed in the area of plasticity to efficiently model and predict stress-strain curves. Metals generally experience linearly elastic stress-strain relationships up to the proportional limit. Beyond this limit, the stress-strain relationship becomes nonlinear and exhibits a power-law type response, but will remain elastic until the yield point is reached. Figure 2.4 illustrates this behavior.

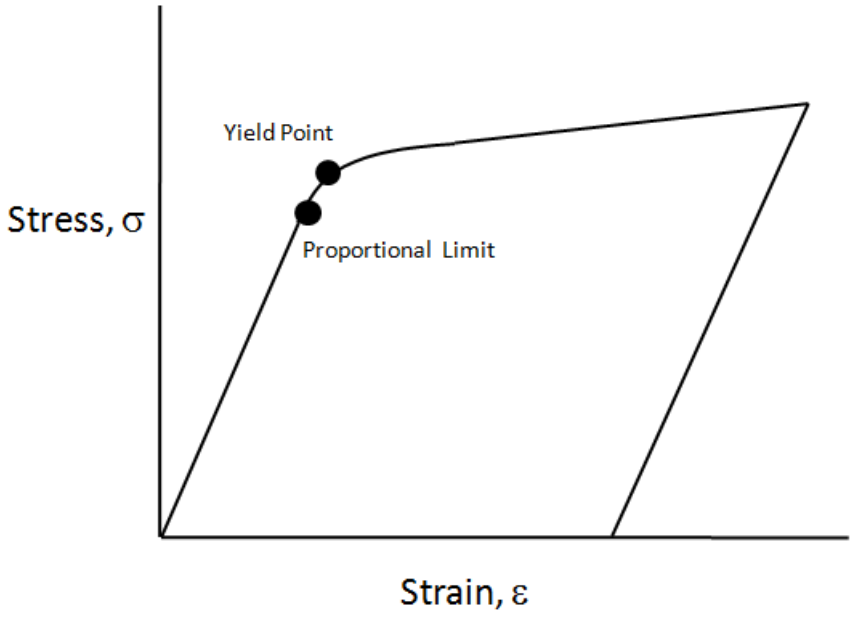

Figure 2.4: Stress-strain curve

Plasticity models require flow and hardening rules as well as a yield point. The flow rule defines the relationship between stress and plastic deformation, while the hardening rule characterizes the type of work hardening, either isotropic of kinematic hardening, that is experienced by the material.

Isotropic hardening is characterized by a uniform increase in yield strength across all directions.From a stress-strain perspective this translates to the compressive yielding being equivalent to the tensile yielding, even after unloading. This implies that the yield surface retains a constant shape while changing in size [13]. This type of hardening is assumed in non-cyclic loading cases because it cannot account for the Bauschinger Effect, which is characterized as the asymmetry between tensile and compressive strengths that becomes more pronounced as the number of cycles increases. Figure 2.5 illustrates this effect, with the typical isotropic and kinematic hardening responses included.

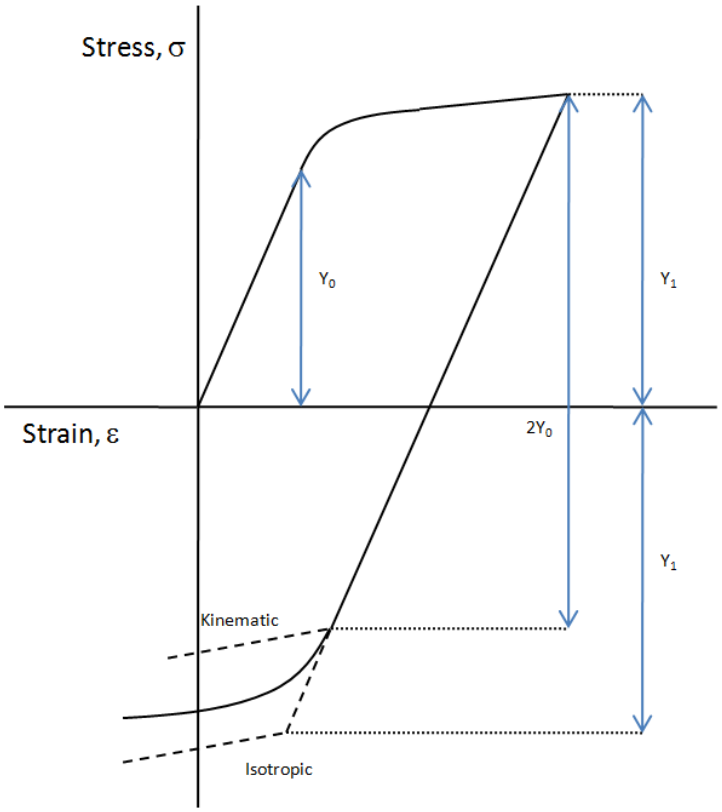

Figure 2.5: Stress-strain cyclic curve illustrating the bauschinger effect

Kinematic Hardening is characterized by an increase in yield strength in the direction of the applied stress. Thus, if the load is tensile, the yield strength will increase in that direction while the compressive strength, which acts in the opposite direction, becomes weaker to compensate. This implies that the yield surface can translate without its size or shape changing [13]. From a stress-strain perspective, kinematic hardening ischaracterized by the elastic range remaining constant throughout the cyclic loading. This allows kinematic hardening to account for the Bauschinger Effect, which makes this type of hardening the most applicable for cyclic loading testing.

There are four reduced-order plasticity models that are used to characterize these stress-strain relationships: Bilinear Isotropic Hardening (BISO), Multilinear Isotropic Hardening (MISO), Bilinear Kinematic Hardening (BKIN), and Multilinear Kinematic Hardening (MKIN).

Bilinear isotropic hardening (BISO) and bilinear kinematic hardening (BKIN)are a reduced-order models in which the nonlinear stress-strain relationship that occurs after yielding is assumed to be linear.Multilinear isotropic hardening (MISO) and multilinear kinematic hardening (MKIN) are reduced-order models that reduce the nonlinear stress-strain relationship that occurs after yielding into a series of linear relationships. For simulations, the multilinear models produce the most accurate results while the bilinear models solve the quickest.

2.5 Reduced-Order Creep Models

Creep is an area of research where reduced-order models are just beginning to develop. The primary reduced-order approach is through a geometrical simplification. This approach focuses on developing a micromechanical model that is inherently comprised of a much smaller

number of unknowns. This micromechanical model is then simulated using eigen-strains that are influenced by eigen-deformations. As the strain is modeled for the micromechanical model, the overall response of the macroscale model is modeled using a reduced-order homogenization [14]. This method was developed to better characterize creep of composites, where micromechanical elements are vital to the whole structure. Because of this, no reduction in solve time was observed.

Some research has been conducted on reducing the solve times of creep simulations. However, this was accomplished through the large time increment (LATIN) method to quickly simulate primary and secondary creep so that tertiary creep simulations, which require the most amount of time to solve, can be executed faster [15]. These authors acknowledges the slow nature of the Newton-Raphson iterative method when applied to nonlinear systems, but sought to reduce the time it took to arrive at the nonlinearities instead of simplifying the nonlinear creep regime itself. As it stands, there is no research being conducted on increasing the efficiency of tertiary creep simulations through a reduced-order constitutive model.

2.6 Literature Review

This section details a thorough literature review on the current trends in creep modeling research and general reduced-order modelsas they are being applied to other fields of research.

The current state of creep modeling research is focused on fine-tuning pre-existing creep models so that specific phenomenon can be accounted for, or on developing novel methods to determine material constants within creep models so that wider experimental parameters can be modeled. Creep models began as simple mathematical formulations that only accounted for

stress. As the field of continuum damage mechanics progresses, increasingly complex phenomenon with increasingly complex variables are being added into creep models so that creep simulations realistically model what is readily observed in experiments.

Temperature-dependence of material constants is a trait that is observed in numerous constitutive creep models and research has been carried out within the last five years to account for it in modern creep models such as the Kachanov-Rabotnov model. To account for temperature-dependence in the Kachanov-Rabotnov model, material constants were analytically or numerically determined fromisothermal creep data. The constants were then plotted against temperature and a mathematical relationship was established by utilizing regression techniques that adequately defined the constant as a function of temperature. In the Kachanov-Rabotnov model, it was determined that the secondary creep constants, *A*, and *n*, and the tertiary damage constant, *M*, exhibited temperature-dependence [12]. The equations that define these relationships are shown in Equations 2.6 through 2.8.

$$A(T) = B\exp\left(\frac{-Q}{RT}\right) \tag{2.6}$$

$$n(T) = \left\langle n_3 T^3 + n_2 T^2 + n_1 T^1 + n_0 \right\rangle + n_{\min} \tag{2.7}$$

$$M(T) = M_1 \exp\left(M_0 T\right) \tag{2.8}$$

Where B, n_i, M_1, and M_0 are material constants, Q is the activation energy, R is the universal gas constant, and T is the temperature. By including the temperature-dependence of the constants

within the modeling routine, a more robust model is established that can calculate material constants for uncharacterized temperatures.

Anisotropy is another phenomenon that is difficult for standard creep models to characterize. In anisotropic materials, the three-dimensional orientation of the grains directly influences the damage evolution. A heavily modified Kachanov-Rabotnov model was developed that incorporated numerousdamage and stress tensor formulations that ultimately resulted in remarkably accurate simulations [16]. The ability to account for grain orientation as well as multiaxial stress states within a high-fidelity simulation is a complex yet novel attribute that makes this modified Kachanov-Rabotnov model extremely robust. However, this level of mathematical characterization can lead to extremely expensive computations.

The Theta-Projection creep model (Equation 2.3) is a poor model to use when long periods of secondary creep are observed. A modified Theta-Projection model was developed that incorporated three terms, one for each creep phase, instead of the normal two [17]. The modified equation is shown in Equation 2.9.

$$\varepsilon_{cr} = \left(\theta_3 \left[1 - e^{\frac{-t}{\theta_1}} \right] + \theta_4 \left[t + \frac{\theta_2}{5e} \left(e^{\frac{t}{\theta_2}} - 1 \right) \right] + \theta_7 \frac{t}{\theta_5} e^{\theta_6 \left(\frac{t}{\theta_5} - 1 \right)} \right) \theta_8 \tag{2.9}$$

This modification allowed for physical meaning to be associated with the coefficients in the new model, which meant that constants could be determined from experimental data. When this modified Theta-Projection model was used to simulate the creep response of a Ni-base superalloy, which is known to experience long secondary creep responses, the results were a large improvement compared to the standard model.

A separate modification was made to the Theta-Projection model solely to develop material constants for the tin-silver alloy that had physical meaning [15].This version of the modified Theta-Projection model is shown in Equation 2.10.

$$\varepsilon_{cr} = A_0\left[1-e^{(-\beta_0 t)}\right]+A\left[1-e^{(-\alpha t)}\right]+B\left[e^{(\alpha t)}-1\right]+B_0\left[e^{(\beta_1 t)}-1\right] \tag{2.10}$$

The goal of the research described in this paper was to fit the modified Theta-Projection model to the data and then to extract the values of the constants to determine experimental parameters such as primary creep rate, the minimum creep rate and the time at which it occurs, and the time to failure. Temperature and stress-dependence relationships of the material constants were also developed. A creep model that has experimentally determined material constants is beneficial in that characteristic creep curves can be readily modeled with minimal use of fitting routines. However, the primary issue with the Theta-Projection model and all of its modificationsare that it cannot be reduced to a linear equation because of the cumulative nature of the individual creep terms. In the case of Equation 2.9, steady-state creep is characterized by adding the secondary and primary creep terms together. The secondary creep term is semi-linear, but becomes nonlinear as time progresses. In the case of Equation 2.3, no secondary term exists and the minimum creep rate is merely an inflection point where creep hardening transitions into creep softening. In both cases this means that a reduced-order constitutive model cannot be developed from the modified Theta-Projection models.

A notable characteristic of constitutive models for creep that are not damage-based is that they fail to adequately capture the tertiary creep response. Figure 2.6 illustrates this using a modified Norton model and a modified Theta-Projection model.

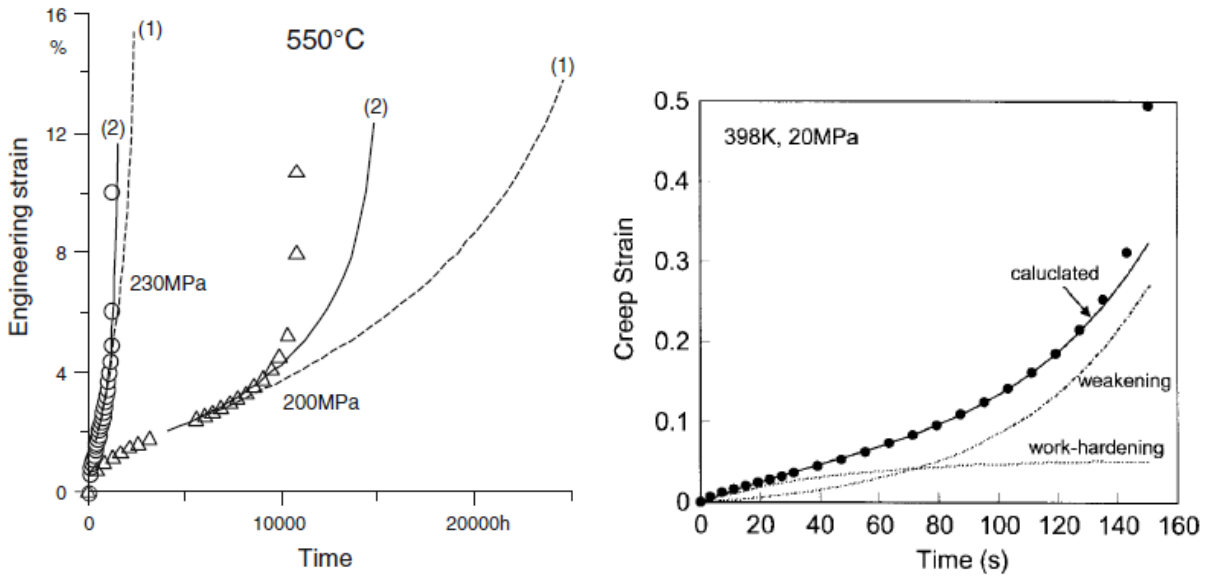

Figure 2.6: Illustration of poor tertiary creep response using (left) modified norton model [18] and (right) modified theta-projection model [15]

Accurately modeling tertiary creep is usually not of interest to designers because components are to be replaced before tertiary creep sets in, as rupture occurs not too long afterwards [17]. In most cases, designers simply use secondary creep models to determine when tertiary creep could begin. However, accurate characterization of tertiary creep is necessary in creep crack growth characterization or in root cause investigations of nuclear reactor or industrial gas turbine components. As such, the development of creep models that can capture the extremely nonlinear behavior of tertiary creep cannot be completely ignored.

Even though the modified Norton law developed by Lim et al.(2011) did not capture the near-rupture portion of tertiary creep, it was still utilized to determine a rule that could be employed to determine the onset of necking, which is the physical manifestation of near-rupture and rupture tertiary creep [18]. This was accomplished by using the Hart instability criterion

[19], which detects deformation instability through the rate of change in cross-sectional area. This criterion is displayed in Equation 2.11.

$$\frac{\ddot{\varepsilon}^{eng}}{\dot{\varepsilon}^{eng}} - 2\frac{\dot{\varepsilon}^{eng}}{\left(1+\varepsilon^{eng}\right)} > 0 \tag{2.11}$$

where ε^{eng} is the engineering strain. Coupling the instability criterion with a modified Norton equation allowed the researchers to accurately predict the change in cross-sectional area up to 75% of the total creep life [18]. If a model that could more accurately capture the near-rupture tertiary creep life were to be coupled with the instability criterion these results could be dramatically improved.

Wen et al. (2013) coupled a modified Kachanov-Rabotnov strain-based tertiary damage model with crack tip stress and strain formulations in an effort to more accurately simulate the influence of cracks in creep of components [20]. Figure 2.7 illustrates the rapid onset of tertiary creep that is characteristic of the investigative material, 316 stainless steel.

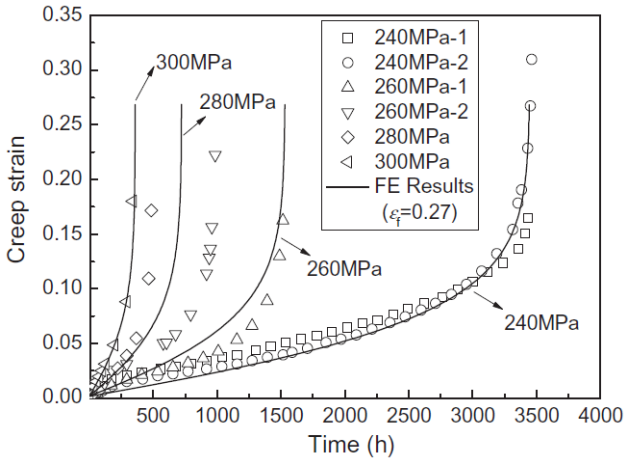

Figure 2.7: Characteristic creep life of 316 stainless steel [20]

It is observed that the modified Kachanov-Rabotnov model is able to predict the rapid onset of tertiary creep. This is an important characteristic because crack growth is influenced by the strain rate in tertiary creep and can even cause tertiary creep to begin earlier than normal because of the reduction in cross-sectional area relative to an undamaged specimen.This characteristic ultimately lead to accurate prediction of creep crack growth as observed in Figure 2.8.

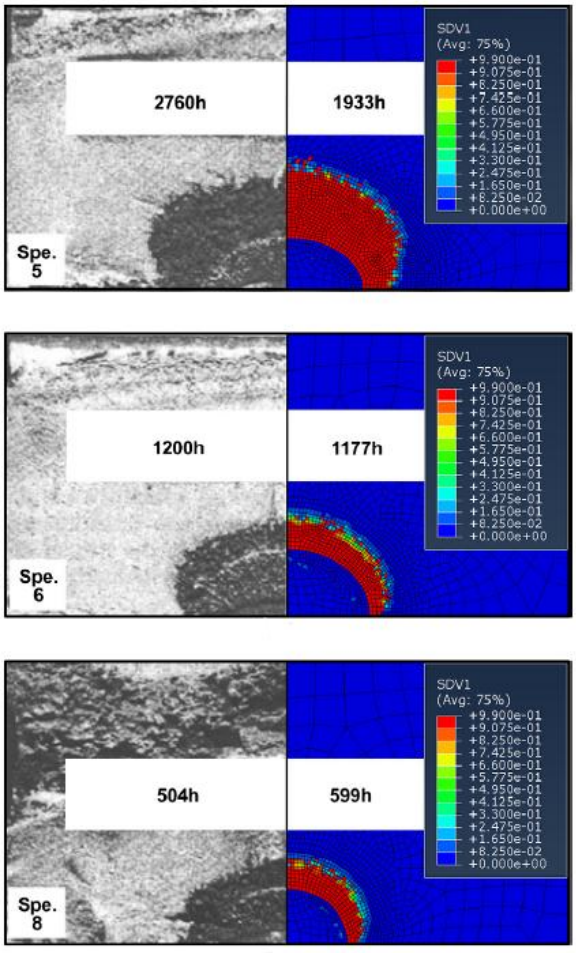

Figure 2.8: Comparison of experimental and simulated results [20]

The work by Zhao et al. (2009) used a separate modified Kachanov-Rabotnov damage model to predict the damage evolution and residual strength of a specimen, which directly correlates to the fracture location. This kind of analysis, as in the modeling of creep crack growth, is dependent on the accuracy of tertiary creep simulations. A genetic algorithm was employed within MATLAB to determine values for the material constants that would produce best-fit creep curves that agreed with experimental data [21]. Figure 2.9 shows the results.

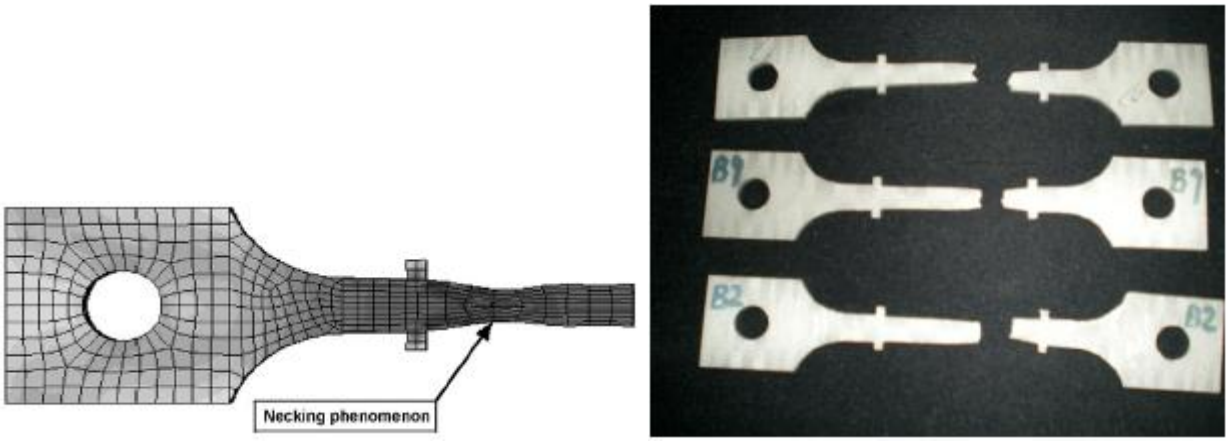

Figure 2.9: Comparison of experimental and simulated results [21]

It is observed that having a model that accurately captures tertiary creep behavior including the near-rupture region is vital in predicting failure.

Reduced-order models are designed to reduce the amount of computational resources that are required to solve a large-scale simulation, while still maintaining a satisfactory degree of accuracy so that necessary results can be ascertained. Two primary approaches that are generally employed to solve this: a reduced-geometry model or a reduced-calculational model. Reduced-geometry models decrease the number of unknowns in a given problem through a simplification

of the experimental model or environment. Some examples of this included reducing a three-dimensional flow field into a series of two-dimensional profiles or a reduction of a three-dimensional material model into an axisymmetric two-dimensional model. Reduced-calculational models are less common, but they seek to reduce the complexity of the problem through physical assumptions that are problem specific. An example of this is the computationally expensive Navier-Stokes compressible equations are replaced with Euler equations, which are computationally simple.

Reduced-order models are implemented heavily in computationally-intensive fields such as aerodynamics and fluid mechanics. Approximations in these fields are generally established through low-accuracy simulations and wind tunnel testing. In recent years there has been a dramatic increase in the use of high-fidelity simulations as quicker and more in-depth analyses are required to develop more efficient designs in a shorter amount of time. With these high-fidelity simulations, computational solve times of multiple days are becoming more commonplace. This is largely because of the inherent complexity of three-dimensional flow fields as well as high Reynolds numbers that complicate the governing Navier-Stokes equations. Alonso et al. (2012) successfully developed a reduced-order models that reduces the solve time from days to minutes. Its primary approach was to reduce the larger problem into a series of smaller problems that are solved independently and then coalesced for a complete analysis. This was accomplished in part by utilizing Euler equations, which are computationally simple, in place of compressible Navier-Stokes equations, which are computationally taxing [22]. This approach is similar to what is explored in this thesis.

Another approach that has been observed in reduced order models involves implanting statistical techniques within pre-existing reduced order models so that a higher degree of accuracy is obtained. Researchers used this concept to add stochastic estimation, mean-square error minimization, and conditional expectations within the OPSTROM reduced-order model to increase the resolution of simulating a nonlinear beam response [23]. This paper was influential because it redeemed the negative aspect of this specific reduced-order models in that it over-emphasized efficiency at the cost of accuracy. Figure 2.10 illustrates the improvement in accuracy compared to the original reduced-order model.

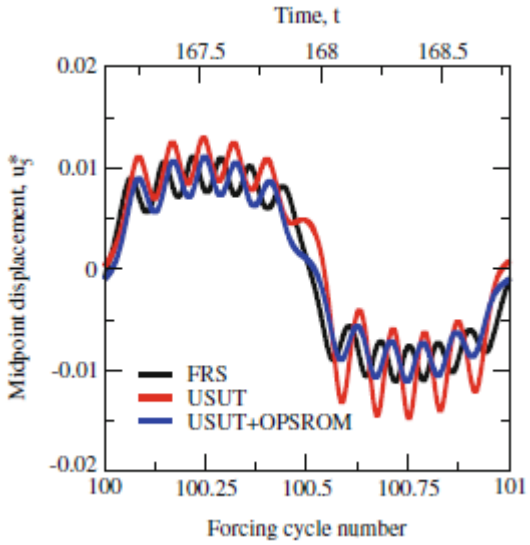

Figure 2.10: Comparison of fully resolved simulation (FRS) amd an under resolved simulation with and without the OPSTROM statistical additions [23]

The increase in solve times because of the added statistical calculations was a necessary trade-off for the sake of accuracy. The ultimate goal of a reduced-order model is to maintain a satisfactory level of accuracy while also reducing the computational resources required to fully simulate and

solve the large problem. This author outlines a possible approach that can be utilized if the proposed reduced-order model that is discussed in this thesis introduces too much error into the creep simulation.

In summary, it has become apparent that the current state of creep characterization and research is focused on accuracy with respect to the primary and secondary creep regimes. This is plausible because most industries that are concerned with creep are only interested in determining when tertiary creep begins, as a part will generally be retired not too long after the onset of tertiary creep. Some structural steels and super alloys, however, exhibit creep lives that are dominated by tertiary creep. If the standard part replacement rules were applied to those steels, parts would be replaced much too soon, thereby wasting resources. Increasing the accuracy of tertiary creep modeling is largely ignored because simulations that involve tertiary creep take exponentially longer than primary and secondary creep simulations because of the extreme non-linear nature of tertiary creep. This thesis proves researchers will be able to simulate the entire creep life including near-rupture tertiary creep with a higher degree of accuracy in an exponentially shorter amount of time. This will lead to more effort being focused on understanding tertiary creep because simulations can be carried out much more quickly.

Many researchers and designers that are involved with structural steels or superalloys utilize the Kachanov-Rabotnov model [12, 14, 16, 20, 21]. The Kachanov-Rabotnov model has proven itself to be the best candidate for modeling tertiary creep because of the damage phenomenon that it introduces. Damage, ω, is a number that classifies the state of the microstructure of the material, starting at zero and increasing towards one, which correlates to

rupture. Tertiary creep is so non-linear because, in physical terms, the material starts to deform and crack, and these deformations reduce the effective-area of the material, which increases stress and therefore strain rate. This is exactly what the coupled Kachanov-Rabotnov equations characterize because both equations incorporate the current value of damage. As the damage evolves the strain rate and damage rate increase as well. This lends itself to characterizing tertiary creep relatively well. The Kachanov-Rabotnov equation is widely used in creep research because it is simple to implement in a finite element analysis because the strain and damage equations are provided in rate forms.

It was very difficult to find any research that discussed simulation time with respect to creep simulations because simulation time of creep modeling is generally not quantified in literature. Reduced-order models are used in many other fields of research to increase the efficiency of simulations. Reduced-order modeling approaches can vary. In the two papers that explored reduced-order models for creep [14,15], a reduction of geometrical complexity and non-tertiary creep was employed. An aerodynamics-based reduced-order model reduced the mathematical complexity of the simulation through physical assumptions and reduced the geometrical complexity through generalized node locations [22]. A reduced-order model was also developed to model a nonlinear beam response that reduced the complexity of a beam vibration problem by combining a low-resolution algorithm with a statistical optimization routine [23].

After an extensive literature review, there appears to have been no progress in developing a reduced-order creep model by reducing the mathematical complexity of the equations even though in a few papers [12,16] and a monograph on creep [4] it has been stated that the

Kachanov-Rabotnov tertiary model reduces to a secondary model when damage is restricted. No researchers have deduced that it is possible to utilize multiple sets of material constants to increase the strain rate sequentially so as to reduce the tertiary creep regime, which is non-linear and computationally expensive to simulate, to a series of increasing slopes, which are linear and computationally simple to simulate.

Increasing the efficiency of simulations is an important step in this field of research, as increasing demands for accuracy are increasing the amount of computational resources needed. The rate at which creep can be researched and analyzed will increase dramatically as researchers can quickly carry out accurate simulations on their personal desktops. As creep is further researched and understood, the service lives of energy-producing turbines can be more accurately and quickly predicted. This results in fewer resources being wasted in replacing turbine components prematurely or, alternatively, wasting resources to repair other components that were damaged when a part failed before being replaced.

CHAPTER 3: REDUCED-ORDER MODELING APPROACH

This section will explore the assumptions and considerations that influence the reduced order model. The Tangent-Line-Chord (TLC) Model will then be derived and the available test data will be provided.

3.1 Analytical Model Considerations

Nearlyseventy percent of the CPUsolve time in a creep simulation is utilized simulating tertiary creep. The solve time increases exponentially as the strain rate increases because of the mechanics behind the Newton-Raphson solver (Figure 2.3). In later stages of tertiary creep the strain rate reaches such a large magnitude that it can be considered linear. A Kachanov-Rabotnov governed simulation was carried out and the percentage of total time required as a function of time was calculated. The results are shown in Figure 3.1.

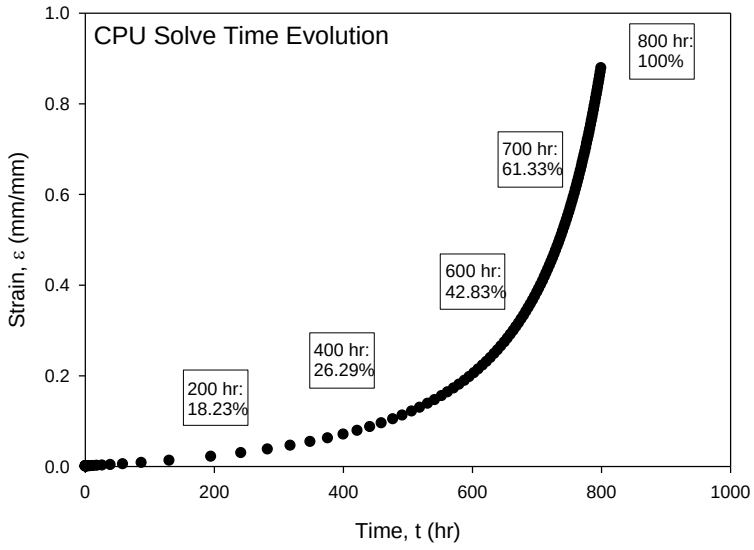

Figure 3.1: Illustration of CPU solve time evolution during creep deformation

It is observed that nearly forty percent of the total solve time was required for the last hundred hours of the eight hundred hour simulation. Visually, tertiary creep begins at roughly five hundred hours, which would place the tertiary creep solve time at nearly seventy percent.

Most finite element solvers have difficulty simulating tertiary creep because they simulate creep using the rate-dependent Newton-Raphson method, which inherently means that finite element solvers can simulate secondary creep very quickly. It is plausible that the required CPU time for creep simulations could be dramatically reduced if the entire creep curve was governed by modified secondary creep, i.e. linear, equations. This is illustrated in Figure 3.2.

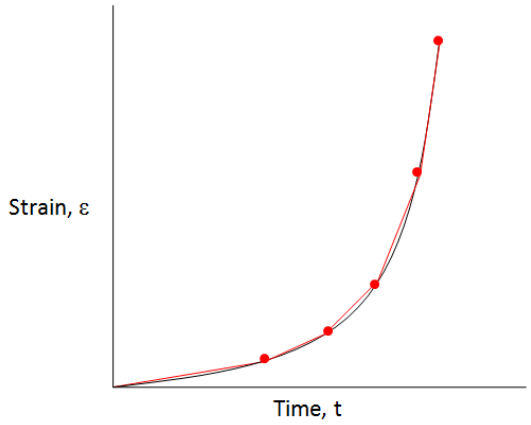

Figure 3.2: Illustration of linear interpolation approach with key data points shown

This concept spurned the creation of a reduced order constitutive model for creep. Any potential reduced-order constitutive creep models willbe limited by the assumption that the slope is always increasing, as well as the error that is induced from an interpolation-based approach. The former limitation becomes an issue when attempting to simulate compressive strain experiments.

Discussed next are the possible mathematical approaches that can be employed to derive the proposed reduced order model.

3.2 Reduced Order Model Approach

Two separate approaches were considered in deriving a reduced-order constitutive model that would adequately characterize tertiary creep: a direct linear interpolation approach and a time-shift interpolation approach.

The direct linear interpolation approach requires that a pre-determined number of data points be chosen so that slopes and ε-intercepts can be calculatedfor as many interpolated lines that are required. Numerical software such as MATLAB simplifies this task greatly with built in interpolation functions. The problem arises when attempting to define the data points, which are illustrated in Figure 3.2, that will be used in the interpolation. Linear interpolation is simple and automatic when an entire data set is used. If the number of interpolants needs to be controlled, then linear interpolation becomes a manual process as the points used for interpolating must be individually chosen. When dealing with large data sets such as in creep experiments,this manual task becomes tedious and more resources are spent preparing the data then what could be saved with a reduced order model. The only way to automate this task is to develop a routine that defines these key data points based on strain rates relative to the minimum strain rate. The main issue with this method is that strain rate histories vary greatly between any two distinct isostress creep curves, even those that involve the same temperature. If the same strain rate relations were used for each creep curve, then the amount of secondary creep equations would not be controllable, which leads to a fluctuation in simulation times and no control over the induced

error. To accurately interpolate the creep curve, strain rate profiles would have to be characterized for each data set to ensure that a controllable number of equations would be produced.

An abstract, but simple approach to implement multilinear modeling is a time-shift based approach. If the original data is time-shifted a predetermined amount, then key points can be determined based on when the secondary creep equations intersect the original and time-shifted creep curves. Mathematically, during primary creep the projected line would chord the original data and be tangent to the time-shifted data. During secondary and tertiary creep, the projected lines would chord the time-shifted data and be tangent to the original data. This approach is illustrated in Figure 3.3.

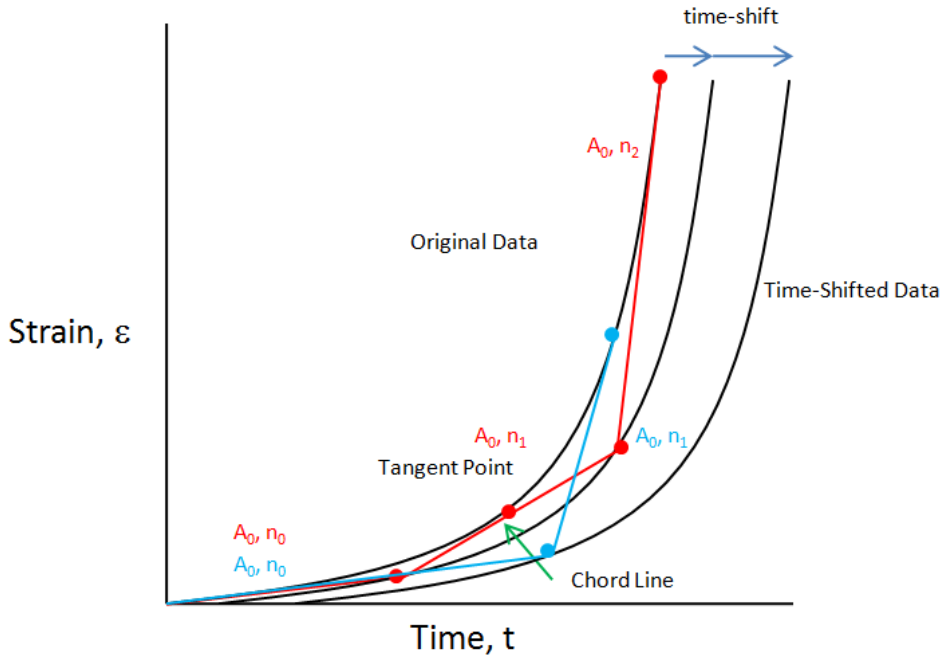

Figure 3.3: Illustration of time-shift data approach

It can be observed that as the time-shift is increased the number of interpolating lines that can be generated decreases. This occurs because larger time shifts result in farther extending interpolated lines that require a higher percentage of total creep time to intersect the opposite curve. A lower number of linesis expected to result in faster solve times at the cost of increased error. As the time shift approaches zero, the amount of error approaches zero and the number of interpolated lines, and therefore the solve time, increases. This quality of the model is useful in that simulations can be executed efficiently while knowing how much error will be introduced. This method is advantageous in that the model generation is not governedbya strain rate relationship as it is in the linear interpolation approach. The lines will numerically follow the curvature of the data as the tangent and chord conditions are numerically solved.

3.3 The TLC Model Numerical Implementation

The TangentLine, Chord(TLC) Model,is derived using novel mathematical manipulations implemented into a multi-paradigm numerical computing environment. The process will be discussed in this section and the routine implemented in MATLAB will be included in the appendices.

The TLC approach relies on an existing creep deformation curve. As previously discussed, the model works well on any material response, however, creep histories that are dominated by tertiary creep are modeled with the most benefit.The existing creep deformation curve is established by an interpolation routine using the creep strain rate formulation of the Kachanov-Rabotnov model, Equation 3.1, with known material constants. This equation is the substitution of the damage rate, Equation 2.5, into the strain rate formulation, Equation 2.4.

$$\dot{\varepsilon}_{cr} = A\left(\frac{\sigma}{\left[1-(\phi+1)M\sigma^{\chi}t\right]^{\frac{1}{\phi+1}}}\right)^{n} \tag{3.1}$$

The advantage of the this latter approach is that the final model can be utilized to correlate material constants and for parametric analyses. If a data-based approach were utilized instead of interpolation, accurate individual fits would be generated, but it would be costly to generate models that correlate over multiple stresses and temperatures because of the strain rate profile process that was discussed earlier.

A channel for the TLC interpolation is developed by time-shifting the creep curve so that appropriate tangent lines and chords can be determined. Numerically, this is accomplished by simply creating a new data matrix where the time values are equal to the original values plus the set time-shift, and the strain values are equal to the original creep curve. The time-shift can be in either the positive or negative direction. It is feasible that positive or negative strain-shifts could also be utilized, but the same effect would be observed as with the time-shift. In most Ni-base superalloys, secondary and tertiary creep regimes dominate the component life [24,25]. In such cases, every line generated by the TLC model will be tangent relative to the original creep curve and will chord the time-shifted creep curve. If a negative time-shift is utilized, then the opposite relations would be observed. When primary creep is present, some lines will be generated that will be tangent to the time-shifted curve and will chord the original creep curve. This is due to the concave nature of primary creep that is characterized by a decreasing strain rate and the convex nature of tertiary creep that is characterized by an increasing strain rate.

Numerically, the initial tangent line is generated by projecting a line that has a slope equal to the mean slope of the original secondary creep data points, which is mathematically represented in Equation 3.2.

$$\dot{\varepsilon}_{proj} = \frac{1}{n}\sum_{i=1}^{n}\frac{\varepsilon_{n+1} - \varepsilon_n}{t_{n+1} - t_n} \tag{3.2}$$

where ε_{proj} is the projected creep strain, ε is the original creep strain, and t is time. When this initial projected line numerically intersects the time-shifted creep curve, i.e. the difference between the projected line and the time-shifted creep curve equals a set tolerance value close to zero, ideally on the order of 10^{-3}, then the time and strain values that correspond to that intersection are stored. A new line is then projected from that location until it intersects both the original and time-shifted creep curves. The intersection of the original creep curve corresponds to the tangent point and the subsequent intersection of the time-shifted creep curve ensures that the generated line is also a chord. If the original curve is not intersected at any point along the projection, the slope of the projected line is slightly increased and the process is iteratively repeated until those conditions are met. This process continues until neither creep curve can be intersected or the slope exceeds 1.0mm/mm/hr. In the first case, the end of the creep data is reached and in the second case rupture is assumed. A complete TLC analysis will produce a figure such as the one observed in Figure 3.4.

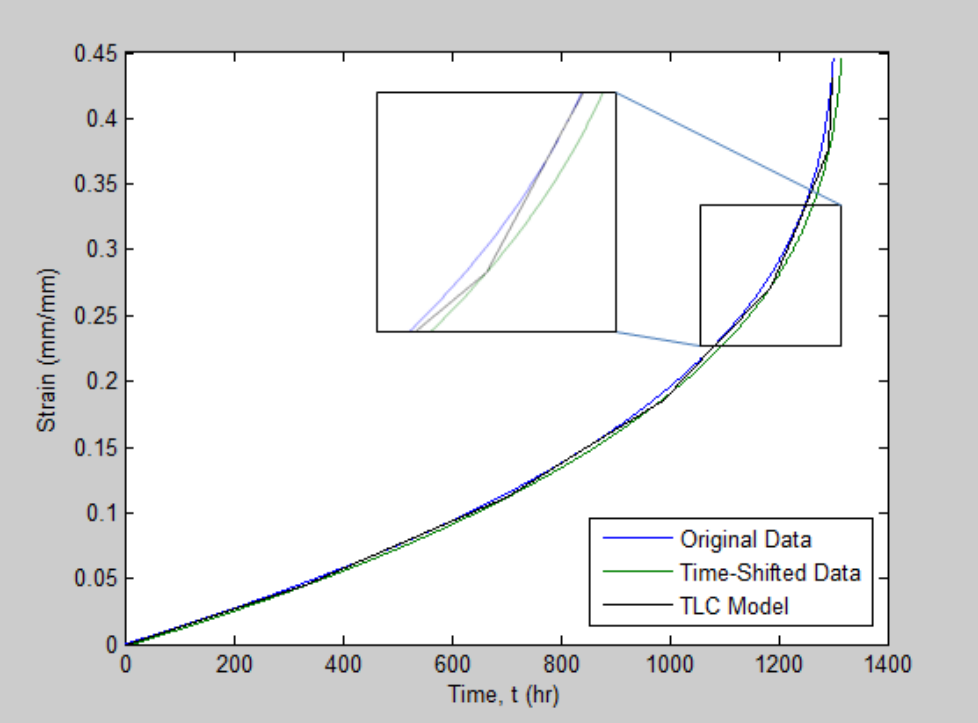

Figure 3.4: TLC generated plot using MATLAB with a time shift of 15 hours

The percent errors between the final time and strain are also calculated relative to the original data using Equations 3.3 and 3.4.

$$SE(\%) = \left(\frac{\varepsilon_{final,original} - \varepsilon_{final,TLC}}{\varepsilon_{final,original}} \right) \cdot 100 \tag{3.3}$$

$$RE(\%) = \left(\frac{t_{final,original} - t_{final,TLC}}{t_{final,original}} \right) \cdot 100 \tag{3.4}$$

These error metrics were only used to ensure that the generated TLC model adequately captured the near-rupture strain history. The size of the time shift influences the amount of overall error,

but in some cases a larger time step can result in a smaller difference in final strains and times relative to a smaller time shift. This is illustrated in Figure 3.5.

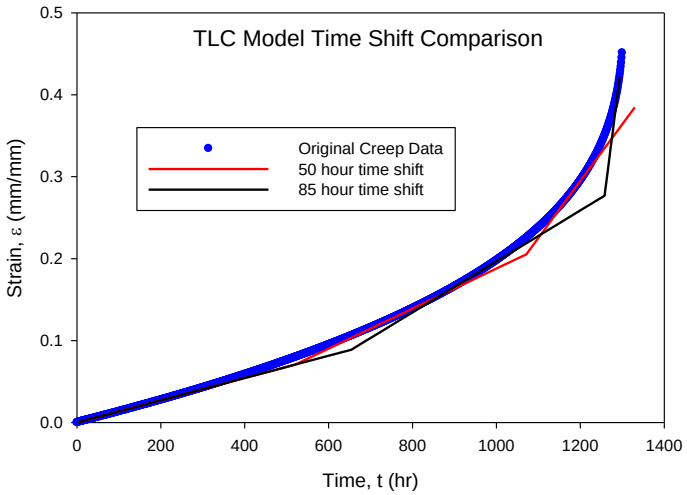

Figure 3.5: TLC model illustrating the effect of the time-shift

In this figure, a time shift of 85 hr resulted in a final strain error or 6.54% and a runtime error of 0.46%, whereas the 50 hr time shift resulted in a final strain error of 14.76% and a runtime error of -2.31%. However, as stated earlier, the 85 hr time shift is less accurate in every other aspect. This is an aspect of the proposed model that must be taken into consideration when applying it to creep prediction.

Knowing that the derivative of the Kachanov-Rabotnov damage model is simply the Norton model, Equation 2.2, it is necessary to calculate the material constants that will generate each subsequent TLC line. The two possible approaches to this are to assume that *A* is constant and that *n* changes with each line, or that *A* changes and *n* remains constant. Both methods facilitate the desired result of an increasing slope, and because both constants exhibit the same

level of stress and temperature dependence [12], either method is plausible. For this research, the former method was arbitrarily chosen. To calculate each *n*, Eq. 3.5 was used, which is the Norton equation manipulated to solve for *n*.

$$n_i = \frac{\log\left(\frac{\dot{\varepsilon}_{cr}}{A}\right)}{\log(\sigma)} \tag{3.5}$$

Here, *n* is the Norton constant for the TLC line that has slope equal to $\dot{\varepsilon}_{cr}$. The number of *n* constants will change depending on the magnitude of the time shift used. In Figure 3.5, the 50 hr time shift resulted in five different values for *n* and the 85 hr time shift resulted in four different values for *n*. If material constant was the variable to be solved for in each TLC increment, then Equation 3.6 would be used.

$$A_i = \frac{\dot{\varepsilon}_{cr}}{\left(\sigma^n\right)} \tag{3.6}$$

For a single creep curve, the TLC Model MATLAB program saves the resulting *n* values, the time range of each TLC line, and the testing parameters (stress and temperature), to text files. These files are then input into the ANSYS software environment. Using the input files that are provided in the appendices, a 1-D element was successfully simulated. The process as a whole was designed to be as automated as possible. Once the Kachanov-Rabotnov material constants and the testing parameters are entered into the MATLAB routine and a TLC model is generated, the user simply needs to run the provided input file to carry out a TLC model driven simulation.

3.4 Available Test Data

Creep data are available for some generic Ni-base superalloys used in turbine engines, where high stresses and temperatures are experienced. These superalloys are unique in that they exhibit creep lives that are dominated by secondary and tertiary creep, such as the creep curve shown in Figure 3.1. Two generic polycrystalline Ni-base superalloys, referred to as Alloy A and Alloy B, will be simulated using the TLC Model. These alloys were chosen because both the Norton and Kachanov-Rabotnov material constants are known for these materials in the corresponding testing parameters. The available data for both superalloys will be shown in Figures 3.6 through 3.13.

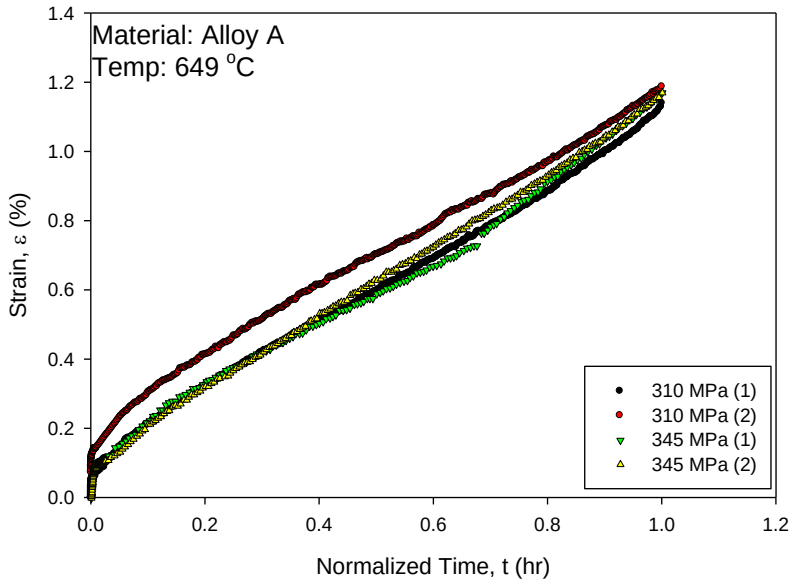

Figure 3.6: Normalized creep curve for alloy A at 649°C

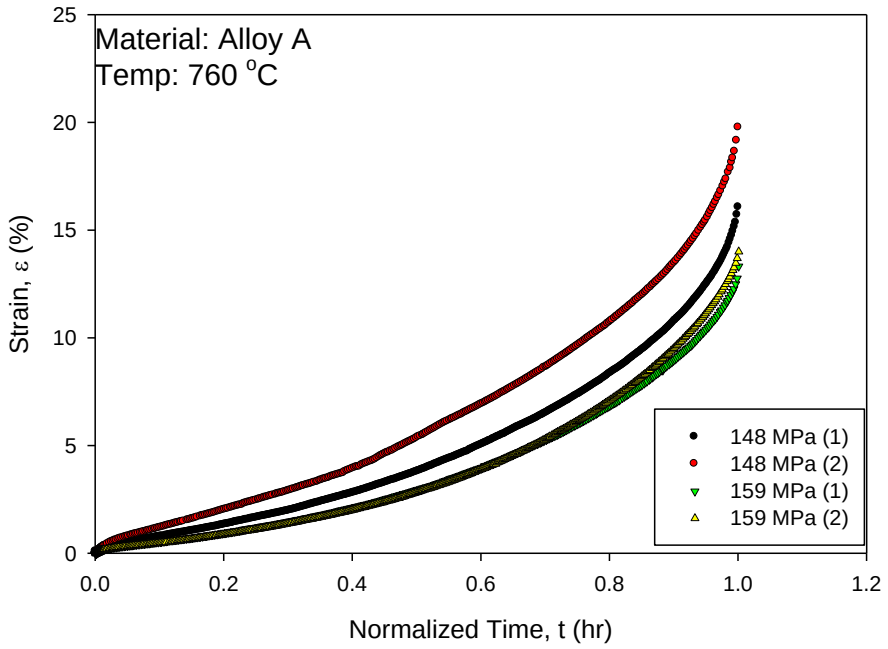

Figure 3.7: Normalized creep curve for alloy A at 760°C

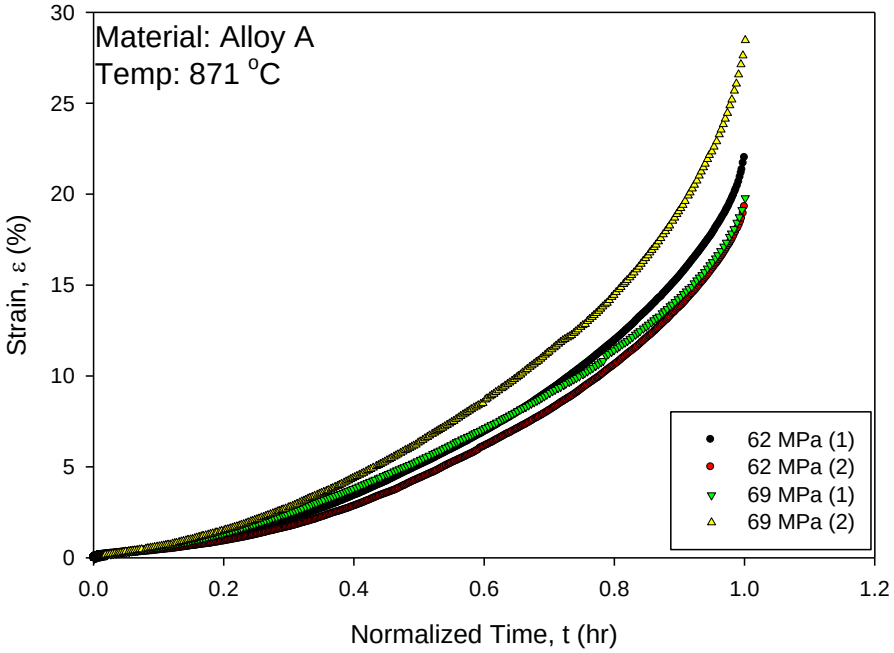

Figure 3.8: Normalized creep curve for alloy A at 871°C

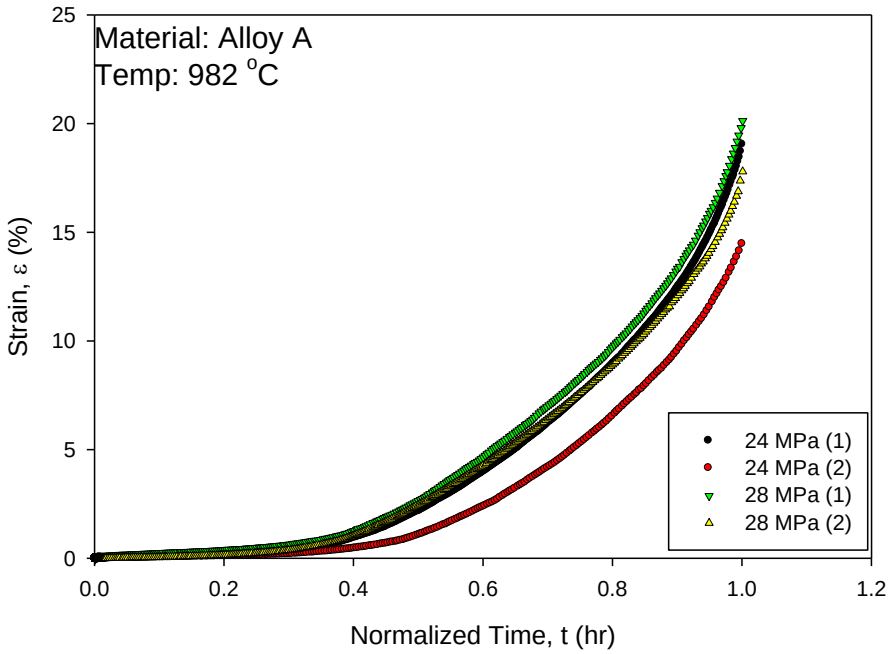

Figure 3.9: Normalized creep curve for alloy A at 982°C

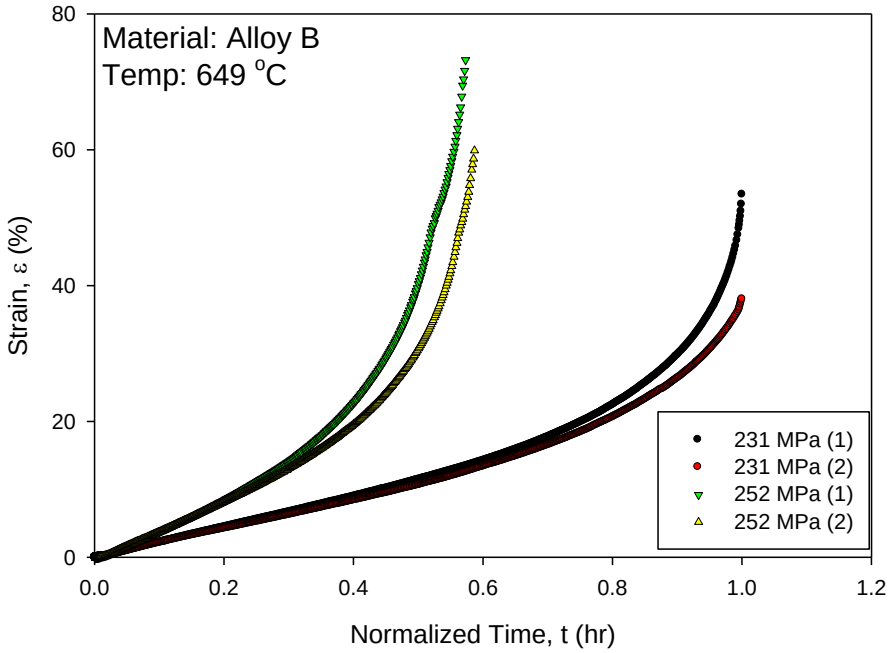

Figure 3.10: Normalized creep curve for alloy B at 649°C

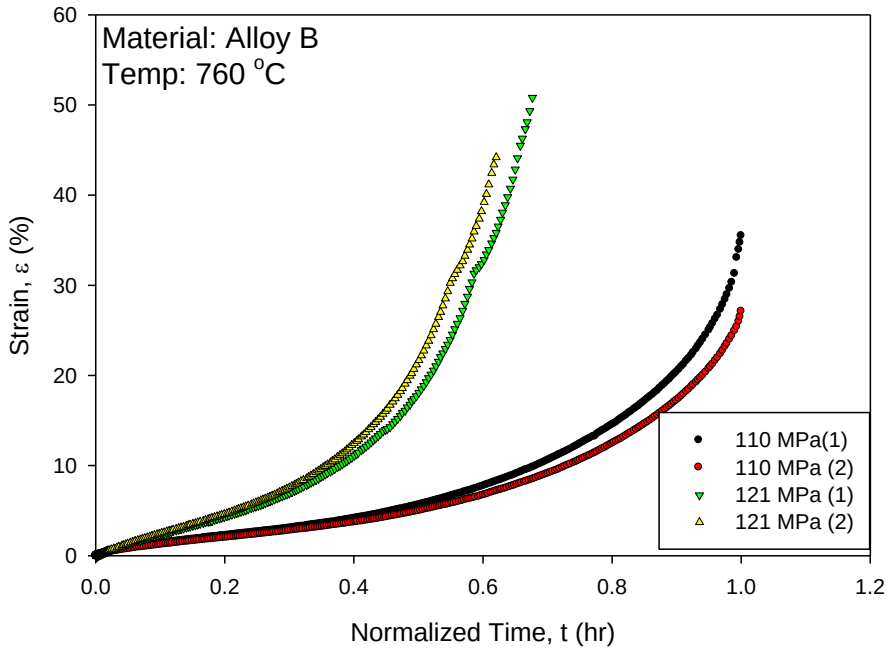

Figure 3.11: Normalized creep curve for alloy B at 760°C

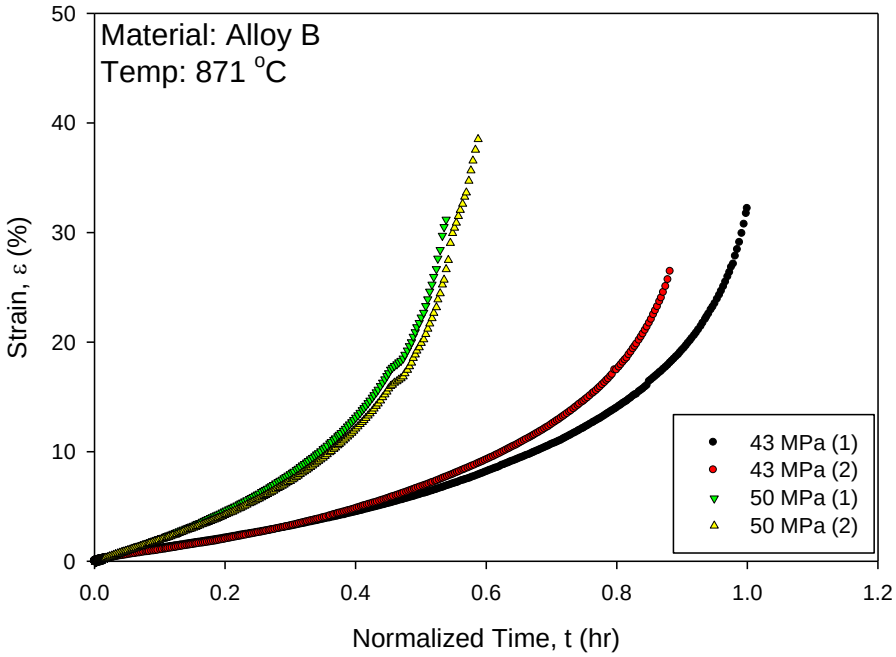

Figure 3.12: Normalized creep curve for alloy B at 871°C

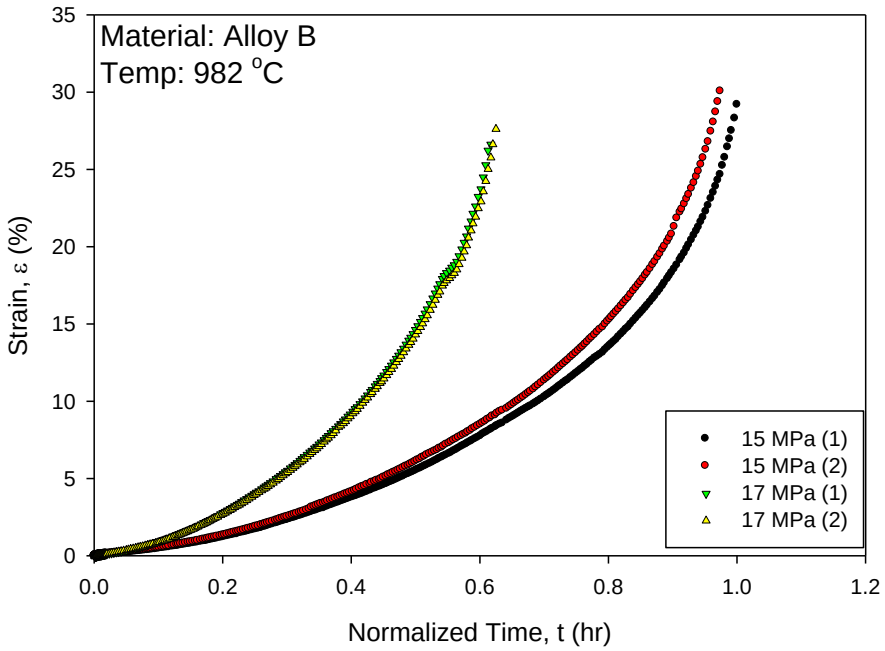

Figure 3.13: Normalized creep curve for alloy B at 982°C

CHAPTER 4: VALIDATION

This chapter provides a parametric analysis of the TLC model including effects of stress and time-shifts as well as the results of the TLC model in terms of its correlation to experimental data.

4.1 Parametric Analysis

Generally, parametric analyses are carried out to determine the effect that certain parameters will have on a system,model,etc. This can also be conducted for analysis of constitutive model behavior. Some examples of a parametric analysisinclude varying stress, temperature, strain rate, etc. with regard to creep behavior. Stress and temperature can be varied to determinehow each parameter influences the model. Because this model is a first generation approach, explicit temperature dependence is not yet included within the model, and is instead incorporated in the material constants. An analysis will be carried out to model the effect of stress because of its natural inclusion within the Norton equation, as well as the affect that the time-shift has on the TLC model .Figure 4.1 confirms that the model reacts to different levels of stress realistically.

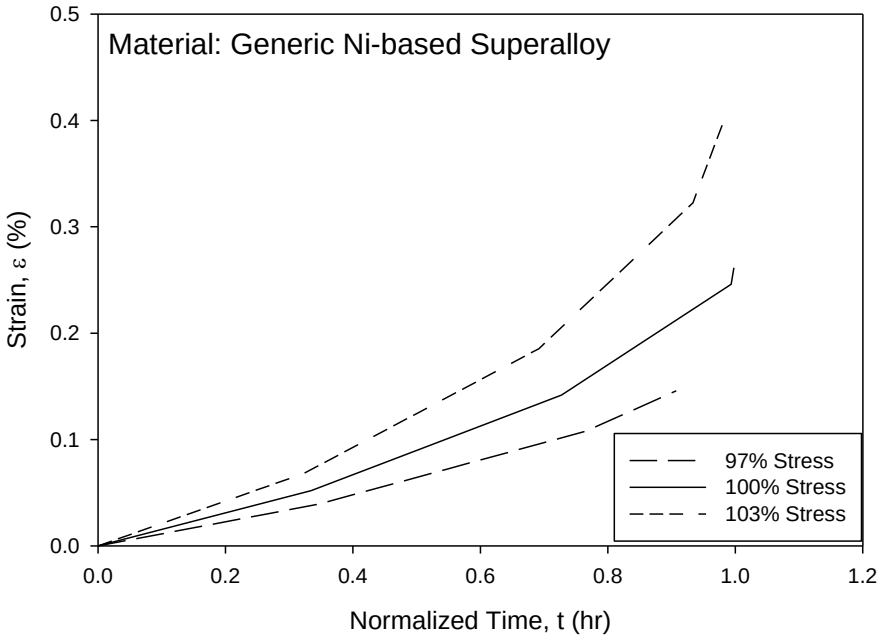

Figure 4.1: Parametric analysis illustrating correct response to changes in stress

The material constants were fixed for each stress case. Strain histories correlated correctly with changes in stress. A small change in stress were used because the material constants are extremely sensitive, as a 10% increase in stress can produce a strain history that is several orders of magnitude higher than the default strain history. This again emphasizes the importance of using accurate constants when creating the Kachanov-Rabotnov interpolated data.

Another influential parameter in the TLC model is the time shift that determines the amount of TLC increments that are generated. In Figure 3.5 it is observed that the size of the time shift directly influences how accurately the TLC model fits the Kachanov-Rabotnov data, both as a whole and in terms of the final strain value. Set values of 3%, 6%, 9%, 12%, and 24%time shifts were applied to four sets of data, each characterized by a different stress and temperature, to determine any possible trends. Figure 4.2, summarizes the results.

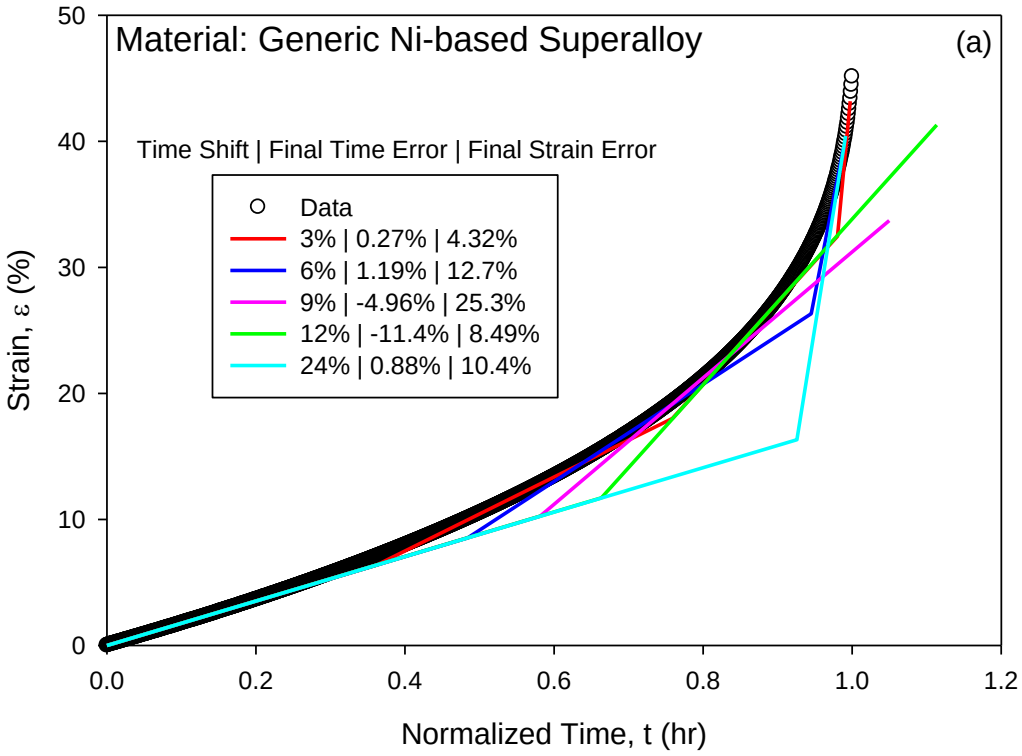
Material: Generic Ni-based Superalloy
(a)
Time Shift | Final Time Error | Final Strain Error
Data
3% | 0.27% | 4.32%
6% | 1.19% | 12.7%
9% | -4.96% | 25.3%
12% | -11.4% | 8.49%
24% | 0.88% | 10.4%
Strain, ε (%)
Normalized Time, t (hr)
0
10
20
30
40
50
0.0
0.2
0.4
0.6
0.8
1.0
1.2

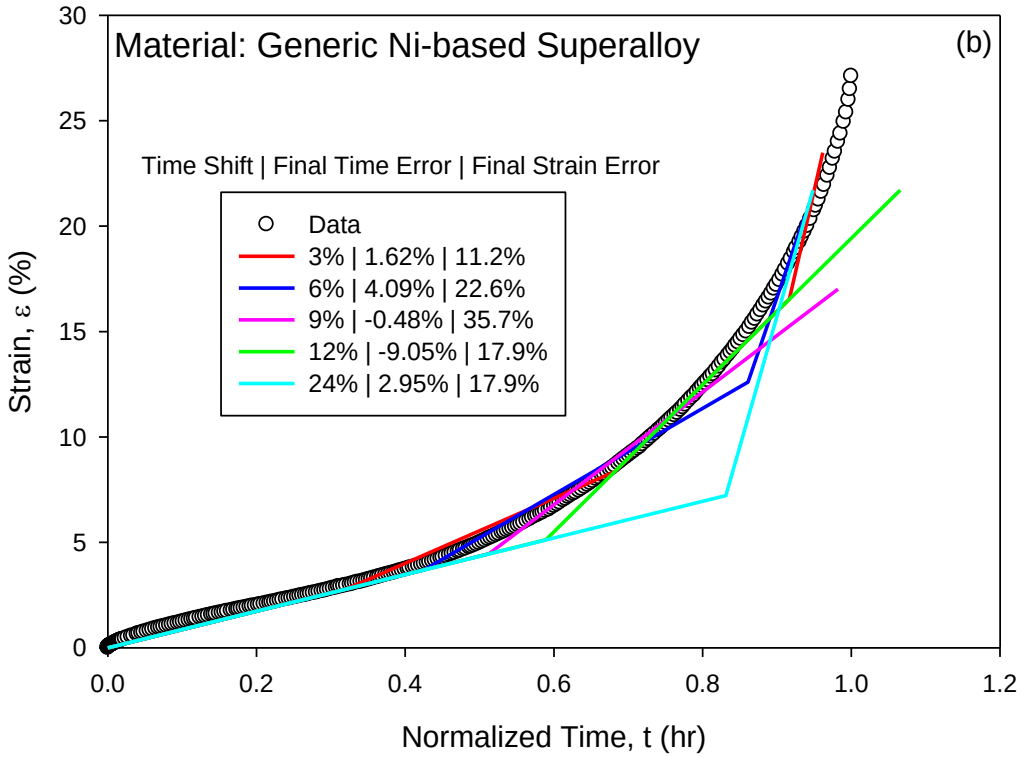
Material: Generic Ni-based Superalloy
(b)
Time Shift | Final Time Error | Final Strain Error
Data
3% | 1.62% | 11.2%
6% | 4.09% | 22.6%
9% | -0.48% | 35.7%
12% | -9.05% | 17.9%
24% | 2.95% | 17.9%
Strain, ε (%)
Normalized Time, t (hr)
0
5
10
15
20
25
30
0.0
0.2
0.4
0.6
0.8
1.0
1.2

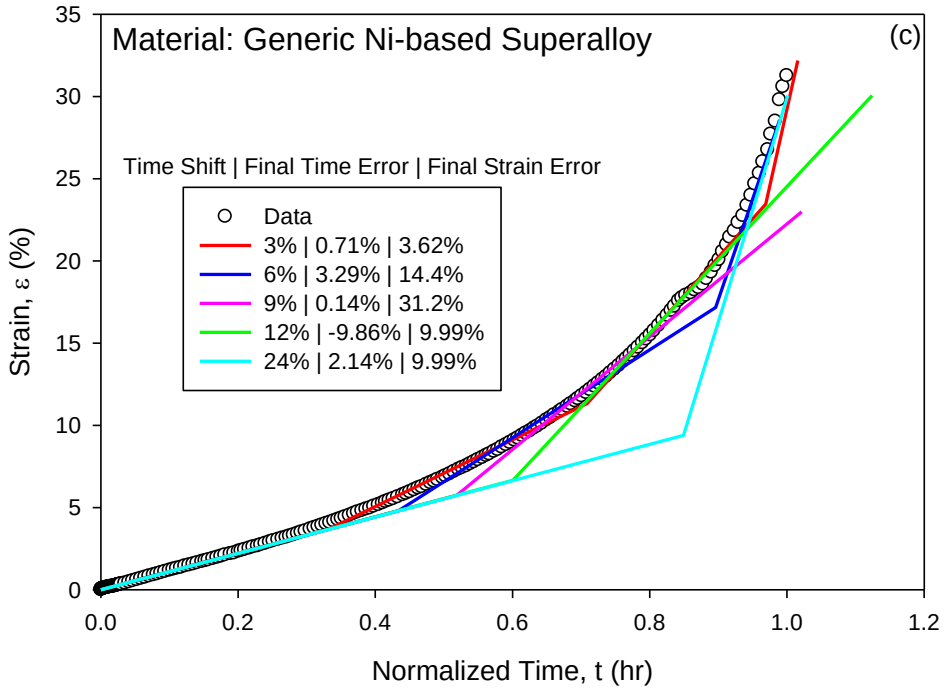

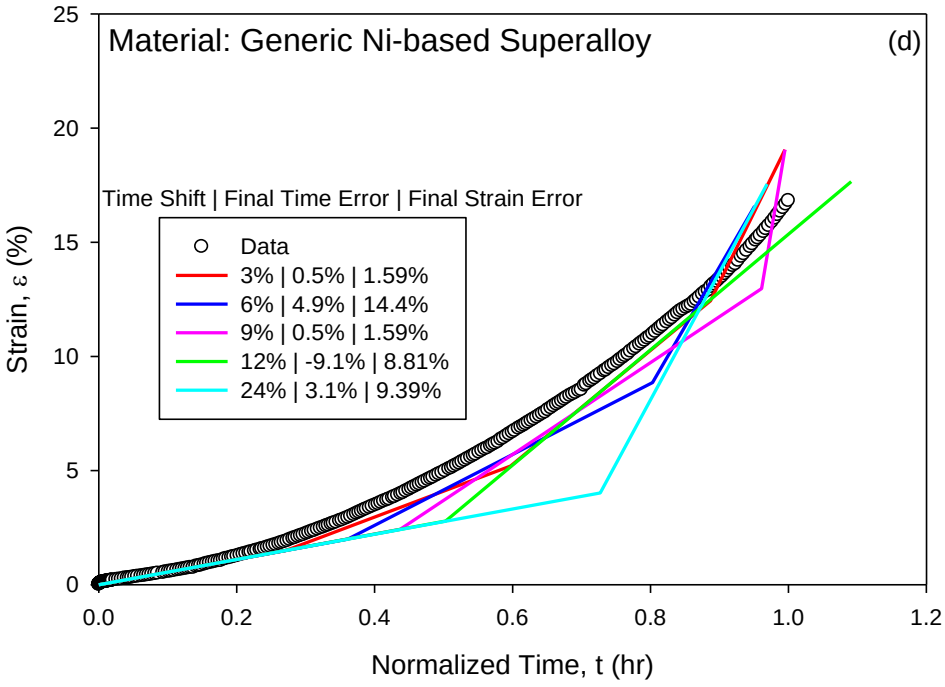

Figure 4.2: Parametric analysis illustrating time-step size affect on four data sets

From these results it is observed that 9% and 12% time shifts produce TLC models that do not adequately characterize the maximum tertiary strain rate or the rupture time. The 24% time shift was able to capture the final strain rate and rupture time with more accuracy, despite having a lower degree of correlation compared to the 9% and 12% time-shifts.

Overall correlation was measured using an area-approximation approach. The area between the data and each curve is numerically calculated by multiplying each successive increment of strain with each successive increment of time. This variable is referred to as the cumulative strain energy (%hr). Table 4.1 summarizes the results for Figure 4.2a, and represent the general trend that is observed between the time-shift and overall correlation.

Table 4.1: Summary of cumulative strain energy as a function of time-shift

Time-Shift (%)	Strain Energy (%hr)
3	17.404
6	21.797
9	24.552
12	26.576
24	50.383

It is now quantified that as the time-shift increases, the overall correlation decreases. With this information it is up to the user of the TLC model to determine whether overall goodness of fit or near-rupture characterization is important for a specific creep simulation.

4.2 Results

Out of the available data, preliminary simulations are carried out with given Kachanov-Rabotnov material constants on a differential element of a dog bone specimen, as seen in Figure 4.3, to determine which data sets would correlate with a high degree of accuracy.

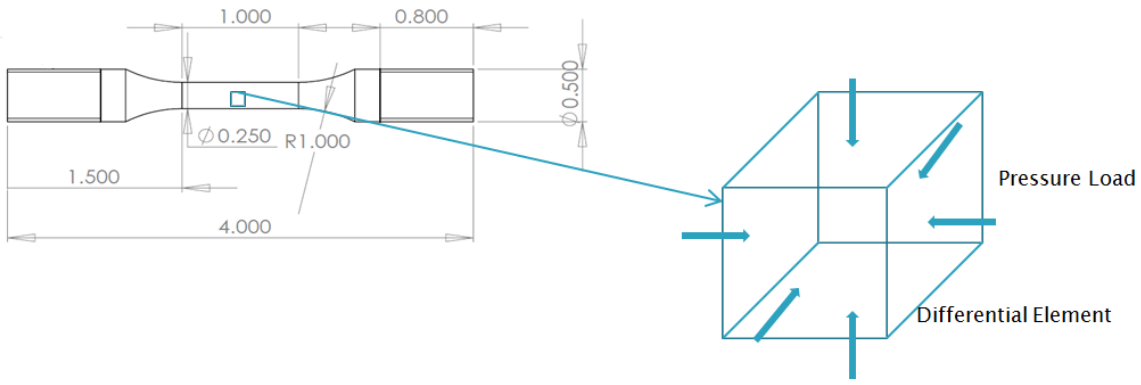

Figure 4.3: Standard tensile specimen geometry (inches) with differential element shown

If the Kachanov-Rabotnov model correlates strongly with the data, then the TLC model will correlate just as well. Because this research is not focused on creating best fit lines, data sets that were not adequately characterized by the given Kachanov-Rabotnov constants were omitted. The results are evaluated based on final strain rate predictions to gauge if the reduced-order model adequately characterized the near-rupture tertiary creep strain rate. Overall correlation was measured using the cumulative strain energy formulation. The TLC model is indicated by the relative time-shift used, with the number of increments generated in parenthesis. Norton model results were included to illustrate how a secondary creep model grossly underestimates the creep life. Simulations were carried out on two cores of a quad-core Intel i5 4.2 GHz processor that was coupled with 8 GB of DDR3 1600 ram. Figures 4.4 through 4.13 summarize the Alloy A results.

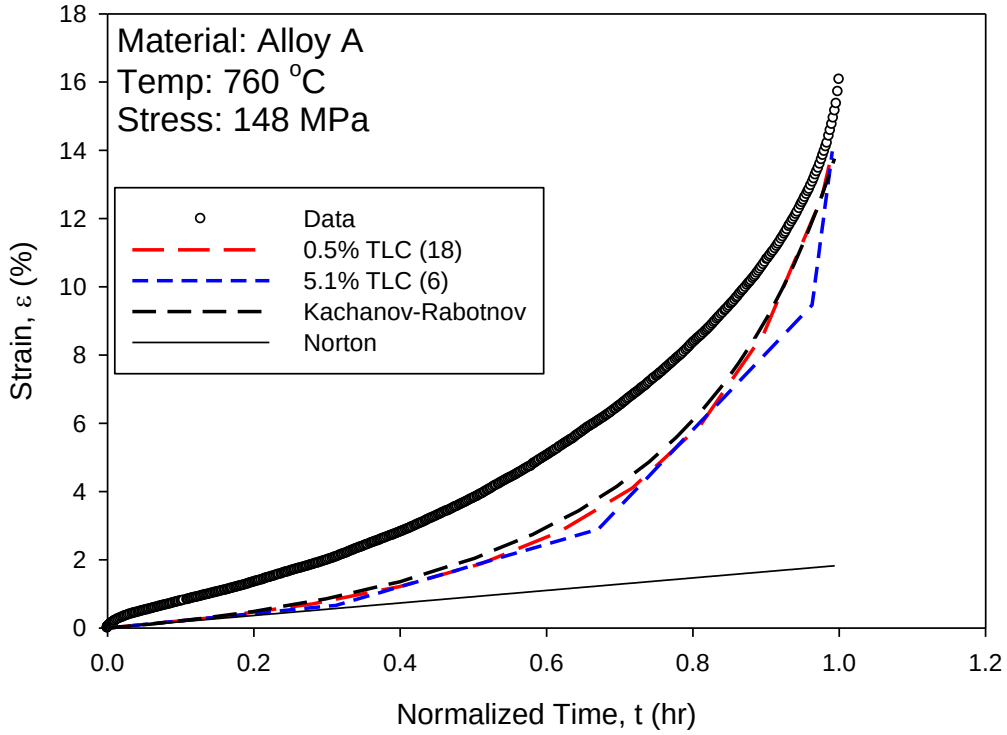

Testing Parameters		Final Strain Rate (%/hr)				
Stress (MPa)	Temp (°C)	Data	0.5% (18)	5.1% (6)	KR	Norton
		0.201	0.096	0.167	0.065	0.002
148	760	Cumulative Strain Error (%hr)				
		5.1% (6)		Norton	KR	
		1763		4620	1550	

Figure 4.4: Alloy A creep modeling results for 148 MPa at 760°C

For the 148 MPa data set, the strain rate at rupture was 0.201 %/hr. The 18 increment TLC model predicted a final strain rate of 0.096 %/hr while the 6 increment TLC model predicted a final strain rate of 0.167 %/hr. The Kachanov-Rabotnov model predicted a final strain rate of 0.065 %/hr while the Norton model predicted a final strain rate of 0.0019 %/hr. The cumulative strain energy for the TLC model was 13.74% worse than the Kachanov-Rabotnov model.

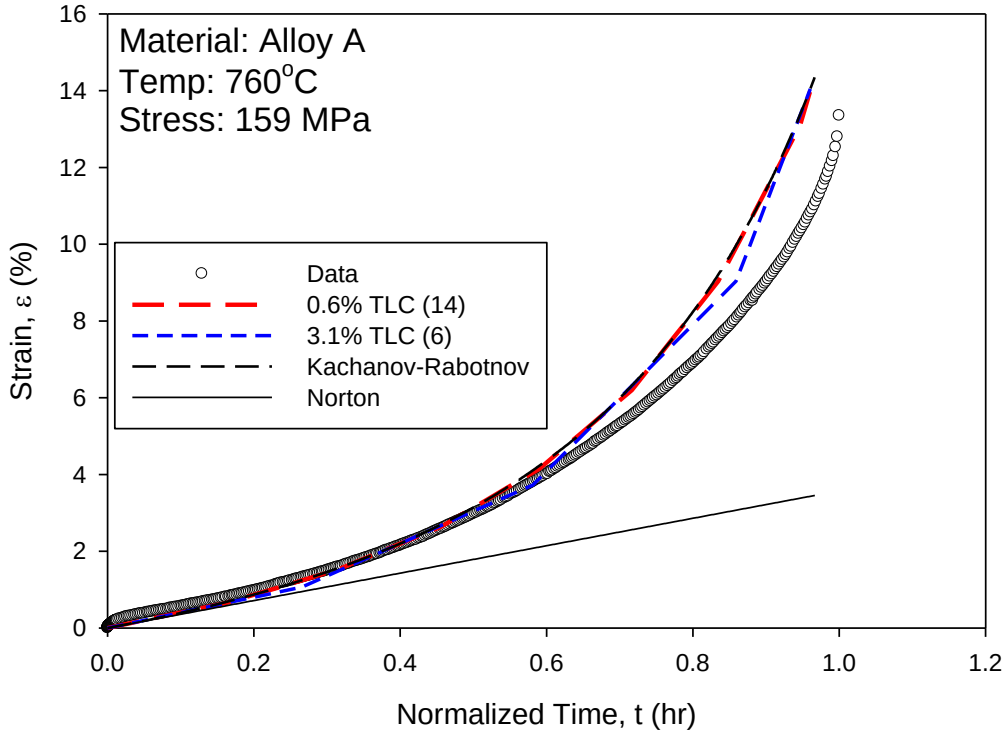

Testing Parameters		Final Strain Rate (%/hr)				
Stress (MPa)	Temp (°C)	Data	0.6% (14)	3.1% (6)	KR	Norton
		0.278	0.078	0.060	0.056	0.004
		Cumulative Strain Error (%hr)				
159	760	3.1% (6)		Norton	KR	
		403		2900	497	

Figure 4.5: Alloy A creep modeling results for 159 MPa at 760°C

For the 159 MPa data set, the strain rate at rupture was 0.278 %/hr. The 14 increment TLC model predicted a final strain rate of 0.078 %/hr while the 7 increment TLC model predicted a final strain rate of 0.060 %/hr. The Kachanov-Rabotnov model predicted a final strain rate of 0.056 %/hr while the Norton model predicted a final strain rate of 0.0043 %/hr. The cumulative strain energy for the TLC model was 18.91% better than the Kachanov-Rabotnov model.

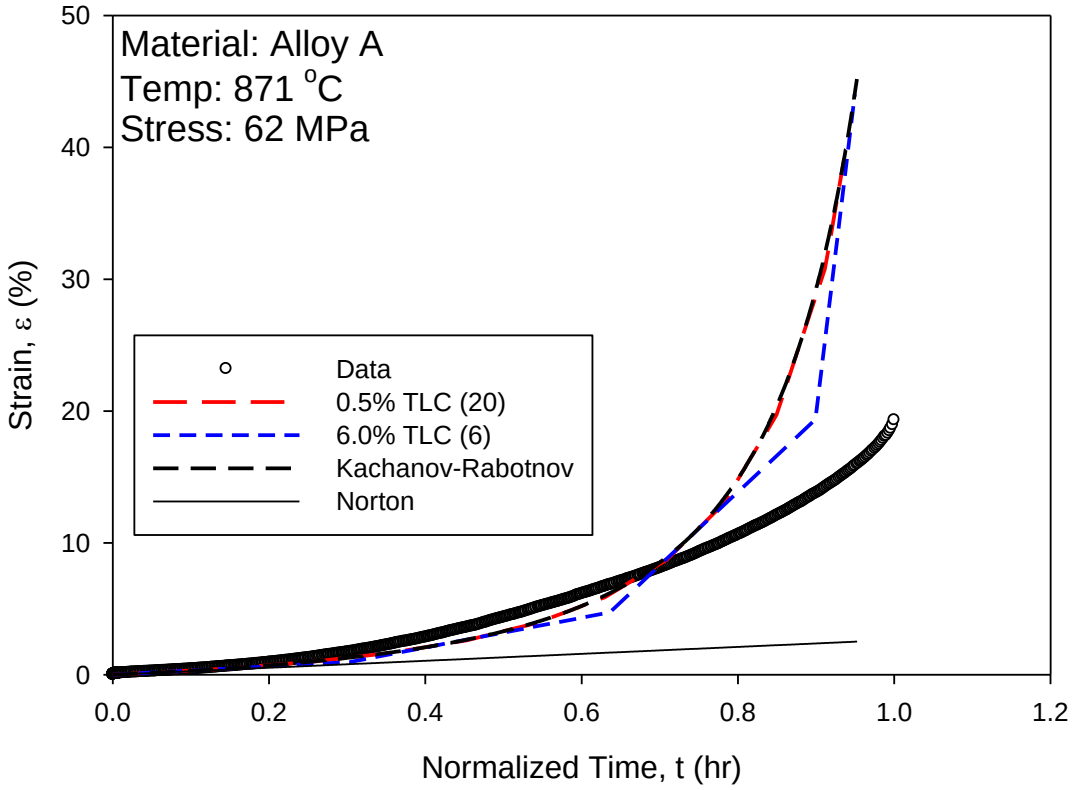

Testing Parameters		Final Strain Rate (%/hr)				
Stress (MPa)	Temp (°C)	Data	0.5% (20)	6.0% (6)	KR	Norton
		0.187	0.323	0.466	0.389	0.003
62	871	Cumulative Strain Error (%hr)				
		6.0% (6)		Norton	KR	
		2090		5160	2685	

Figure 4.6: Alloy A creep modeling results for 62 MPa at 871°C

For the 62 MPa data set, the strain rate at rupture was 0.187 %/hr. The 20 increment TLC model predicted a final strain rate of 0.323 %/hr while the 6 increment TLC model predicted a final strain rate of 0.466 %/hr. The Kachanov-Rabotnov model predicted a final strain rate of 0.389 %/hr while the Norton model predicted a final strain rate of 0.0025 %/hr. The cumulative strain energy for the TLC model was 22.16% better than the Kachanov-Rabotnov model.

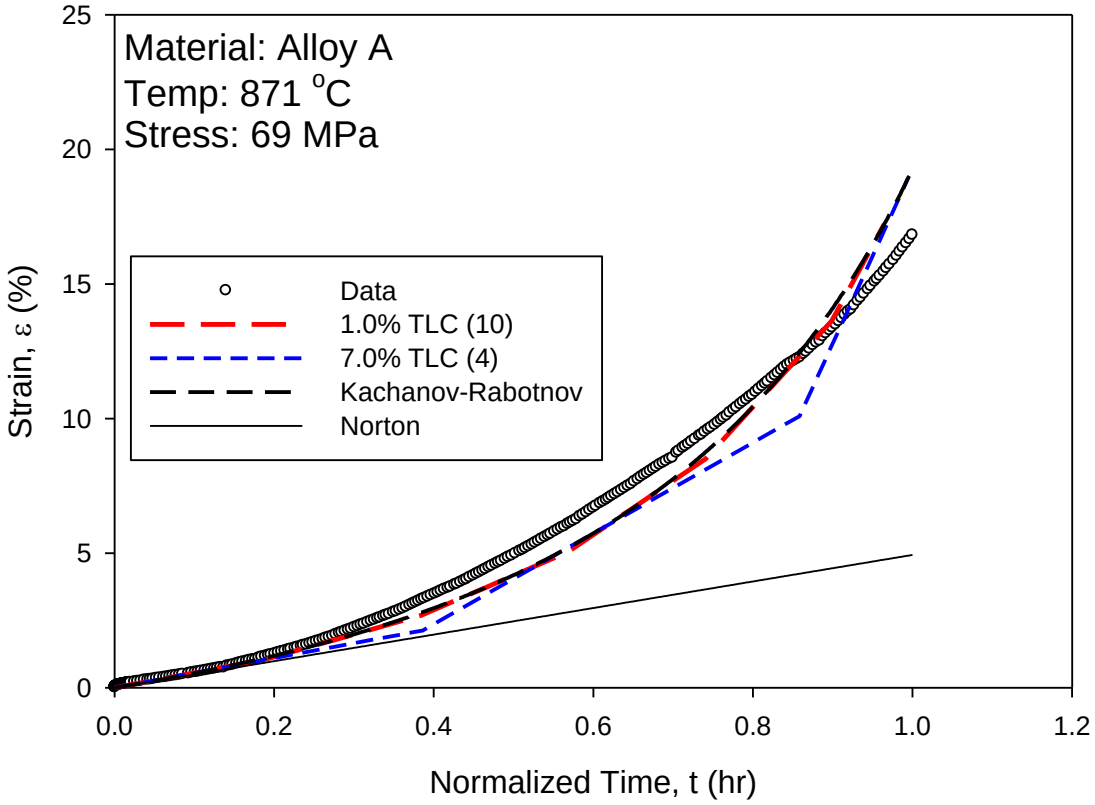

Testing Parameters		Final Strain Rate (%/hr)				
Stress (MPa)	Temp (°C)	Data	1.0% (10)	7.0% (4)	KR	Norton
		0.088	0.109	0.130	0.122	0.010
		Cumulative Strain Error (%hr)				
69	871	7.0% (4)		Norton	KR	
		415		2980	274	

Figure 4.7: Alloy A creep modeling results for 69 MPa at 871°C

For the 69 MPa data set,the strain rate at rupture was 0.088 %/hr. The 10 increment TLC model predicted a final strain rate of 0.109 %/hr while the 4 increment TLC model predicted a final strain rate of 0.13 %/hr. The Kachanov-Rabotnov model predicted a final strain rate of 0.122 %/hr while the Norton model predicted a final strain rate of 0.0099 %/hr. The cumulative strain energy for the TLC model was 51.46% worse than the Kachanov-Rabotnov model.

In summary, these results show that the TLC model excels at characterizing the entire creep response while also capturing near-rupture strain rates of tertiary creep. The overall correlation analysis reveals that the higher time-shift TLC model is the most accurate model when the Kachanov-Rabotnov model is conservative, and is less accurate when the Kachanov-Rabotnov model under-predicts the response. This is the trend that is visually observed in the data. It is also seen that the higher time-shift TLC model shows similar levels of correlation compared to the Kachanov-Rabotnov model when the magnitude of the cumulative strain energy for the Norton model is considered. The TLC model predicts the final strain rates with a higher degree of accuracy compared to the Kachanov-Rabotnov model. When the Kachanov-Rabotnov model overestimated or underestimated the final strain rate, the higher increment TLC models were closer to the actual values in each result. The lower increment TLC model was the most accurate model in regards to final strain rate predictions for the 148 MPa data at 760^{o}C only, and this can be attributed to a unique time-shift that, in a sense, got lucky. The results for Alloy B are shown on the following pages in Figures 4.8 through 4.13.

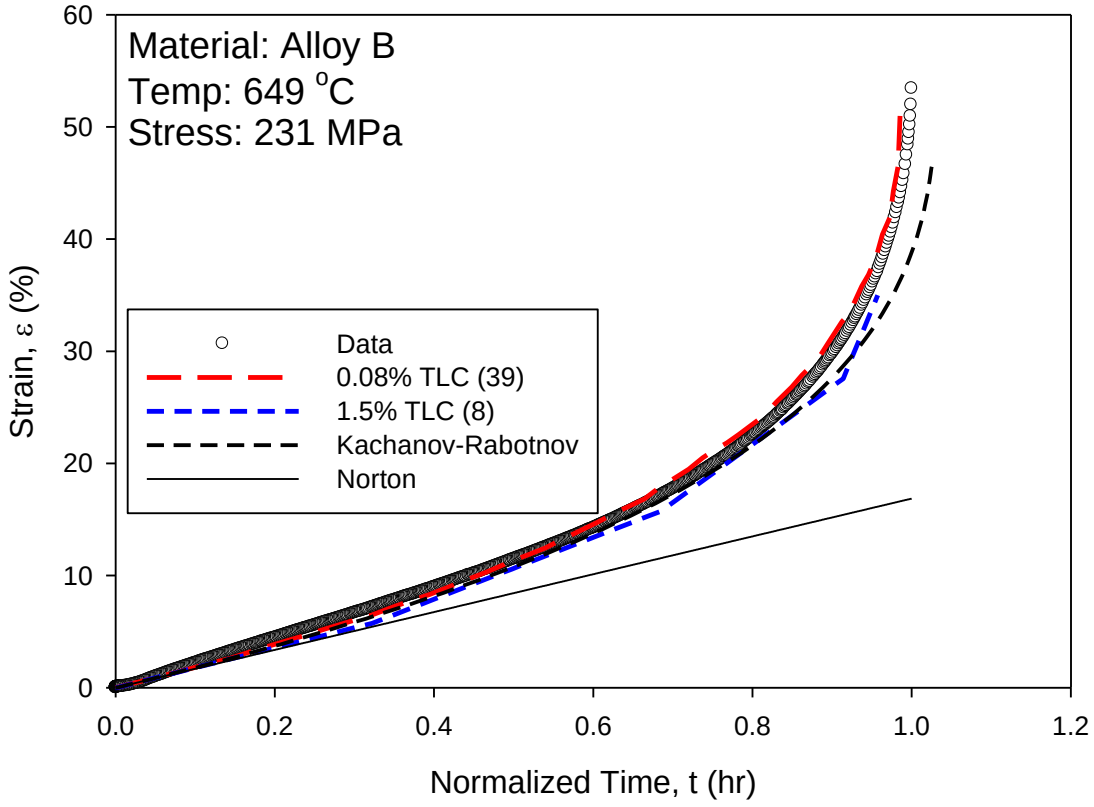

Testing Parameters		Final Strain Rate (%/hr)				
Stress (MPa)	Temp (°C)	Data	0.08% (39)	1.5% (8)	KR	Norton
		1.449	1.504	0.255	0.434	0.013
231	649	Cumulative Strain Error (%hr)				
		1.5% (8)		Norton	KR	
		1305		17560	1072	

Figure 4.8: Alloy B creep modeling results for 231 MPa at 649°C

For the 231 MPa data set, the strain rate at rupture was 1.45 %/hr. The 39 increment TLC model predicted a final strain rate of 1.50 %/hr while the 8 increment TLC model predicted a final strain rate of 0.255 %/hr. The Kachanov-Rabotnov model predicted a final strain rate of 0.434 %/hr while the Norton model predicted a final strain rate of 0.013 %/hr. The cumulative strain energy for the TLC model was 21.74% worse than the Kachanov-Rabotnov model.

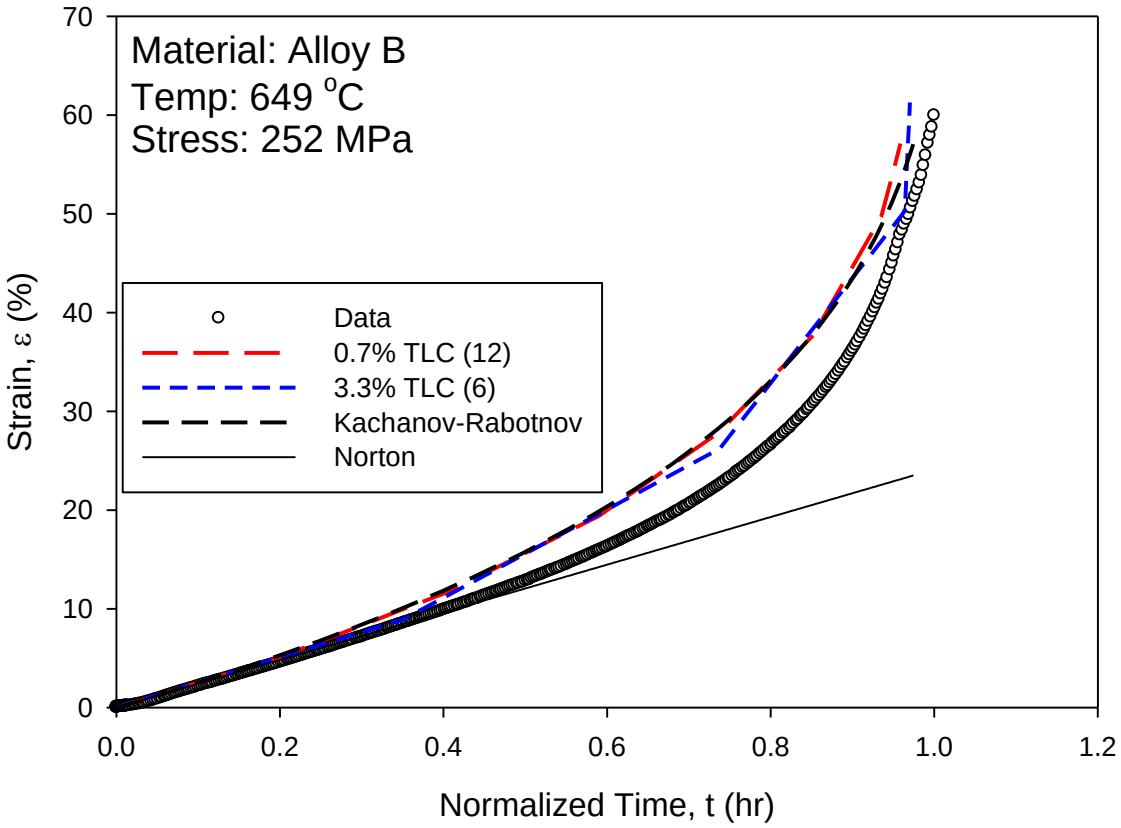

Testing Parameters		Final Strain Rate (%/hr)				
Stress (MPa)	Temp (°C)	Data	0.7% (12)	3.3% (6)	KR	Norton
		0.601	0.411	2.204	0.336	0.031
252	649	Cumulative Strain Error (%hr)				
		3.3% (6)		Norton	KR	
		2062		11400	2632	

Figure 4.9: Alloy B creep modeling results for 252 MPa at 649°C

For the 252 MPa data set, the strain rate at rupture was 0.601 %/hr. The 12 increment TLC model predicted a final strain rate of 0.411%/hr while the 6 increment TLC model predicted a final strain rate of 2.20 %/hr. The Kachanov-Rabotnov model predicted a final strain rate of 0.336 %/hr while the Norton model predicted a final strain rate of 0.031 %/hr. The cumulative strain energy for the TLC model was 21.66% better than the Kachanov-Rabotnov model.

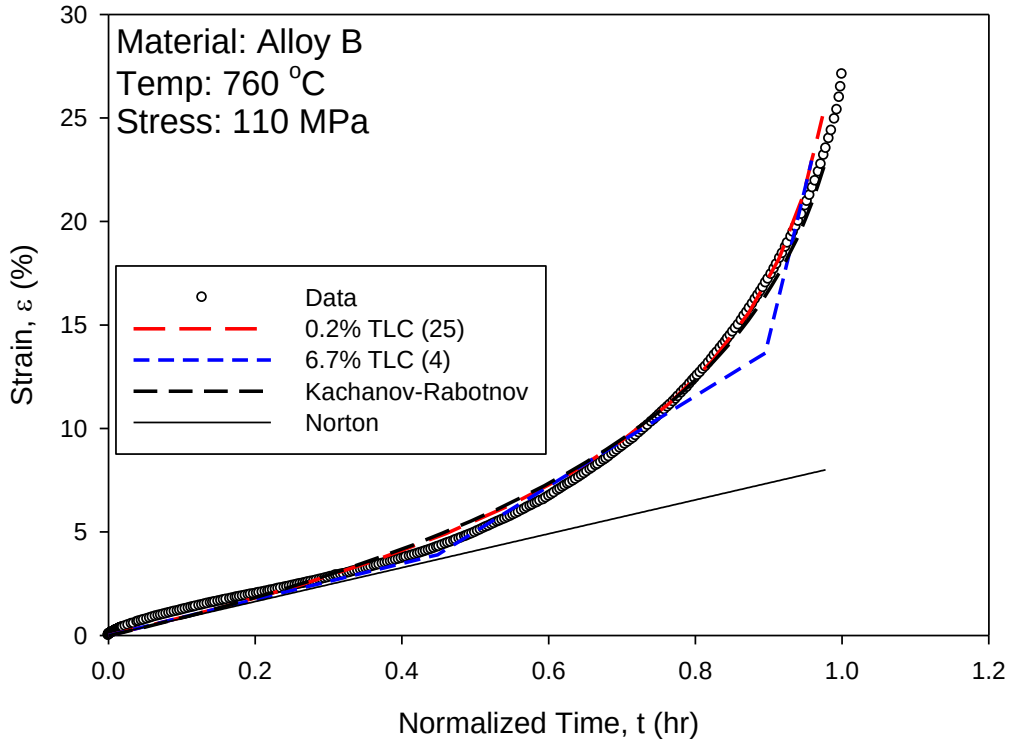

Testing Parameters		Final Strain Rate (%/hr)				
Stress (MPa)	Temp (°C)	Data	0.2% (25)	6.7% (4)	KR	Norton
		0.680	0.268	0.273	0.179	0.015
		Cumulative Strain Error (%hr)				
110	760	6.7% (4)		Norton	KR	
		266		3550	188	

Figure 4.10: Alloy B creep modeling results for 110 MPa at 760°C

For the 110 MPa data set, the strain rate at rupture was 0.680 %/hr. The 25 increment TLC model predicted a final strain rate of 0.268 %/hr while the 4 increment TLC model predicted a final strain rate of 0.273 %/hr. The Kachanov-Rabotnov model predicted a final strain rate of 0.179 %/hr while the Norton model predicted a final strain rate of 0.015 %/hr. The cumulative strain energy for the TLC model was 41.49% worse than the Kachanov-Rabotnov model.

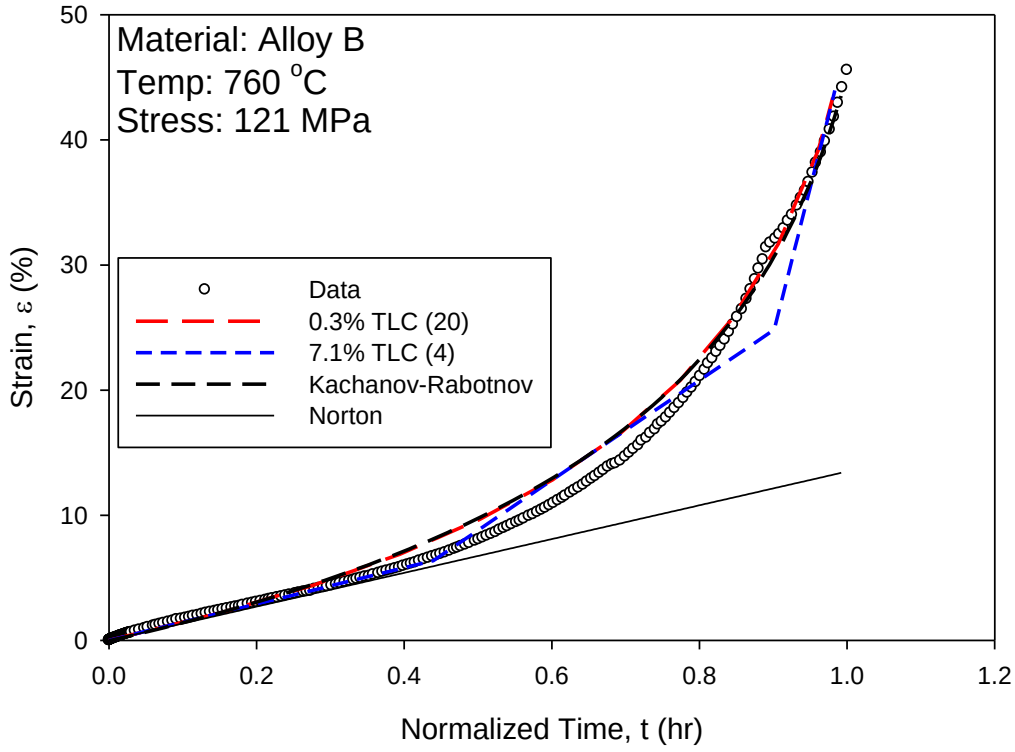

Testing Parameters		Final Strain Rate (%/hr)				
Stress (MPa)	Temp (°C)	Data	0.3% (20)	7.1% (4)	KR	Norton
		0.603	0.606	0.660	0.555	0.038
		Cumulative Strain Error (%hr)				
121	760	7.1% (4)		Norton	KR	
		504		3740	379	

Figure 4.11: Alloy B creep modeling results for 121 MPa at 760°C

For the 121MPa data set, the strain rate at rupture was 0.603 %/hr. The 20 increment TLC model predicted a final strain rate of 0.606 %/hr while the 4 increment TLC model predicted a final strain rate of 0.660 %/hr. The Kachanov-Rabotnov model predicted a final strain rate of 0.555 %/hr while the Norton model predicted a final strain rate of 0.038 %/hr. The cumulative strain energy for the TLC model was 32.98% worse than the Kachanov-Rabotnov model.

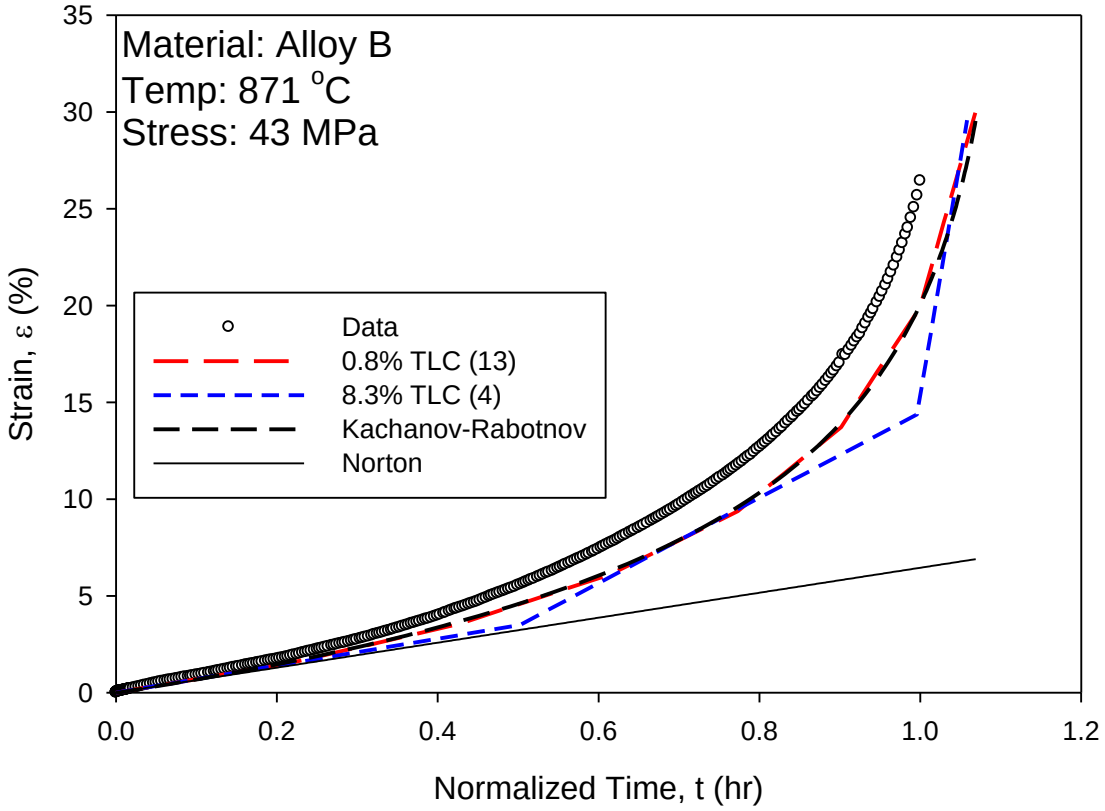

Testing Parameters		Final Strain Rate (%/hr)				
Stress (MPa)	Temp (°C)	Data	0.8% (13)	8.3% (4)	KR	Norton
43	871	0.362	0.258	0.434	0.395	0.011
		Cumulative Strain Error (%hr)				
		8.3% (4)		Norton	KR	
		986		3850	695	

Figure 4.12: Alloy B creep modeling results for 43 MPa at 871°C

For the 43 MPa data set, the strain rate at rupture was 0.362 %/hr. The 13 increment TLC model predicted a final strain rate of 0.258%/hr while the 4 increment TLC model predicted a final strain rate of 0.434 %/hr. The Kachanov-Rabotnov model predicted a final strain rate of 0.395 %/hr while the Norton model predicted a final strain rate of 0.011 %/hr. The cumulative strain energy for the TLC model was 41.87% worse than the Kachanov-Rabotnov model.

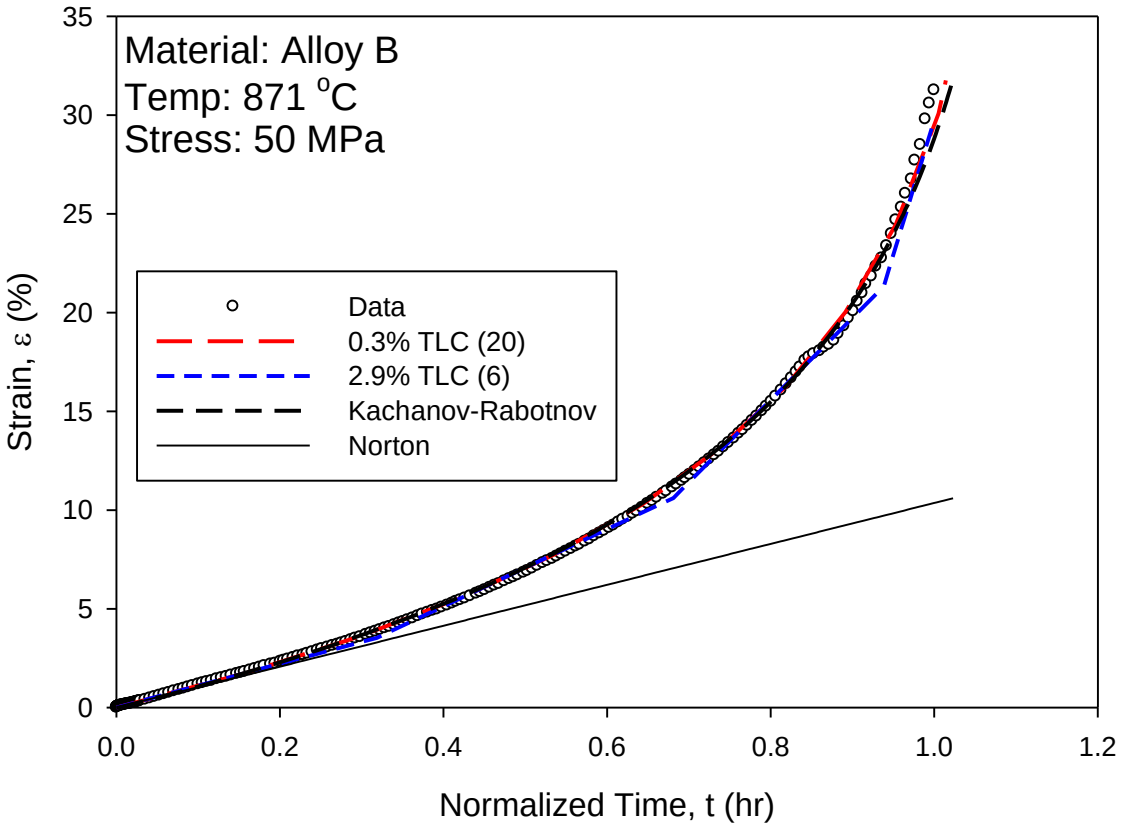

Testing Parameters		Final Strain Rate (%/hr)				
Stress (MPa)	Temp (°C)	Data	0.3% (20)	2.9% (6)	KR	Norton
50	871	0.335	0.559	0.399	0.428	0.030
		Cumulative Strain Error (%hr)				
		2.9% (6)		Norton	KR	
		81		3020	71	

Figure 4.13: Alloy B creep modeling results for 50 MPa at 871°C

For the 50MPa data set,the strain rate at rupture was 0.335 %/hr. The 20 increment TLC model predicted a final strain rate of 0.559 %/hr while the 6 increment TLC model predicted a final strain rate of 0.399 %/hr. The Kachanov-Rabotnov model predicted a final strain rate of 0.428 %/hr while the Norton model predicted a final strain rate of 0.03 %/hr. The cumulative strain energy for the TLC model was 14.08% worse than the Kachanov-Rabotnov model.

In summary, these results again illustrate that the TLC model is nearly just as accurate as the Kachanov-Rabotnov model. The same trend between the overall correlation of the TLC model and the conservativeness of the Kachanov-Rabotnov model is observed for Alloy B. It is also observed again that the TLC model is more accurate in regards to characterizing the near-rupture tertiary creep. The results for the 871^{o}C data were in favor of the Kachanov-Rabotnov model over both the higher and lower increment TLC models. For the 649^{o}C data set, the lower increment TLC model dramatically underestimated and overestimated the near-rupture strain rate while the higher increment TLC model was the most accurate. For the 760^{o}C data set, the lower increment TLC model was the most accurate at the 100 MPa stress level and the higher increment TLC model was the most accurate at the 121 MPa stress level.

CHAPTER 5: BENCHMARKING

This section analyzes the effectiveness of the TLC model with respect to the amount of CPU time that was required to completely solve the creep simulation. Simulations were carried out on a differential element of a dog bone specimen, as illustrated in Figure 4.3. All simulations were executed on two cores of a quad-core Intel i5 4.2 GHz processor that was coupled with 8 GB of DDR3 1600 ram. In each table, the first two models represent the time-shift as a percentage of rupture time with the number of resulting increments in parenthesis.

5.1 Comparison with Secondary Creep Model

Secondary creep models are utilized when a swift and rough approximation of creep is desired. The TLC model, in both higher and lower increments, was simulated alongside the Norton secondary creep model to analyze how the theoretical increase in solve time compares to the degree of accuracy achieved when using the TLC model. Table 5.1 summarizes the results for Alloy A. The number in parenthesis indicates the number of increments used in the TLC model.

Table 5.1: Summary of benchmark results for Alloy A comparing TLC model to secondary creep model

Testing Parameters		CPU Time (sec)		
Stress (MPa)	Temp (^{o}C)			
		0.5% (18)	5.1% (6)	Norton
148	760	47.891	25.172	13.844
		0.6% (14)	3.1% (6)	Norton
159	760	39.922	26.562	13.641
		0.5% (20)	6.0% (6)	Norton
62	871	54.703	25.359	13.938
		1.0% (10)	7.0% (4)	Norton
69	871	32.828	20.797	13.969

From these results it is apparent that the CPU solve time required to solve the TLC-driven creep simulation is directly influenced by the number of TLC increments that are used. The Norton secondary creep model can be considered a one increment TLC model, so the similar times that are observed for each Norton simulation are consistent with theory. At first, it appears that the higher increment TLC models solve in a more efficient amount of time because of the ratio between the number of increments and the solve time. However, when the time required to ramp the load in the simulation is taken into account (~12 seconds) and subtracted from all of the benchmark results, it was determined that the average CPU time required for each TLC increment is 1.7 seconds. It should be noted that the Norton model and TLC model both used the same automatic time-stepping parameters for ramping the load, which can be seen in the input files found in Appendix A. The time difference between the TLC and Norton models can be considered negligible when one considers the dramatic increase in accuracy that the TLC model produces compared to the Norton model. Table 5.2 summarizes the benchmarking results between the TLC and Norton models for Alloy B.

Table 5.2. Summary of benchmark results for Alloy B comparing TLC model to secondary creep model

Testing Parameters		CPU Time (sec)		
Stress (MPa)	Temp (^{o}C)			
		0.08% (39)	1.5% (8)	Norton
231	649	75.172	26.469	13.25
		0.7% (12)	3.3% (6)	Norton
252	649	34.516	22.844	13.031
		0.2% (25)	6.7% (4)	Norton
110	760	54.031	19.969	13.422
		0.3% (20)	7.1% (4)	Norton
121	760	50.812	20.062	13.469
		0.8% (13)	8.3% (4)	Norton
43	871	37.594	20.531	13.562
		0.3% (20)	2.9% (6)	Norton
50	871	52.094	24.141	13.719

These results are very similar to the results shown in Table 5.1a. The CPU time required to simulate secondary creep using the Norton model is nearly constant while the TLC model requires an average of 2.0 seconds per increment when factoring out the initial load ramping. The perceived benefit from the fast solve time of the Norton model is again offset dramatically by the degree of accuracy that is achieved with the TLC model. It should again be noted that the automatic time-stepping parameters within the initial loading step are equal between the two input files used for the respective models.

5.2 Comparison with Tertiary Creep Model

Tertiary creep models are utilized when a more thorough and accurate approximation of creep is desired. The TLC model, in both higher and lower increments, was simulated alongside the Kachanov-Rabotnov tertiary creep model to determine whether the solve time can be reduced by a large enough amount to warrant the level of error that is induced with the reduced-order

TLC model. Table 5.3 summarizes the results for Alloy A. The number in parenthesis indicates the number of increments used in the TLC model. In each test the same automatic time-stepping parameters were chosen.

Table 5.3: Summary of benchmark results for Alloy A comparing TLC model to tertiary creep model

Testing Parameters		CPU Time (sec)		
Stress (MPa)	Temp (^{o}C)			
		0.5% (18)	5.1% (6)	KR
148	760	47.891	25.172	70.328
		0.6% (14)	3.1% (6)	KR
159	760	39.922	26.562	64.578
		0.5% (20)	6.0% (6)	KR
62	871	54.703	25.359	158.02
		1.0% (10)	7.0% (4)	KR
69	871	32.828	20.797	86.844

From these results it can be seen that the TLC model solves in a less amount of time than the Kachanov-Rabotnov model in every test. The time required to solve the Kachanov-Rabotnov simulation is directly related to the strain rate evolution that is produced by the material constants. Figures 4.4 through 4.7 reveal that the final strain rate trend correlates with the solve time trend seen in Table 5.3. However, a direct relationship between the ratio of final strain rates and solve times cannot be established from this data alone.

Table 5.4: Summary of benchmark results for Alloy B comparing TLC model to tertiary creep model

Testing Parameters		CPU Time (sec)		
Stress (MPa)	Temp (^{o}C)			
		0.08% (39)	1.5% (8)	KR
231	649	75.172	26.469	72.609
		0.7% (12)	3.3% (6)	KR
252	649	34.516	22.844	86.094
		0.2% (25)	6.7% (4)	KR
110	760	54.031	19.969	81.438
		0.3% (20)	7.1% (4)	KR
121	760	50.812	20.062	101.53
		0.8% (13)	8.3% (4)	KR
43	871	37.594	20.531	139.53
		0.3% (20)	2.9% (6)	KR
50	871	52.094	24.141	118.47

These results further prove the TLC models effectiveness in reducing the solve time required for the simulation compared to the Kachanov-Rabotnov model. The 39 increment, 0.08% time-shift TLC model required more time than the Kachanov-Rabotnov model for the 231 MPa simulation at 649^{o}C. This contradicts the purpose of the reduced-order model, but in this case the TLC model wasdramatically more accurate than the Kachanov-Rabotnov model at capturing the near-rupture tertiary creep. Initially one would infer that the highest magnitude of final strain rate would be for the 43 MPa simulation at 871^{o}C. However, the highest final strain rate is observed for the 121MPa simulation at 760^{o}C. Among isothermal tests the expected pattern is not observed. The 252 MPa simulation at 649^{o}C had a markedly lower final strain compared to the 231 MPa simulation, but it required a longer CPU time. The same trend is seen in the 871^{o}C simulations. As such, no definitive pattern can be established between the Kachanov-Rabotnov final strain rates and solve times.

In summary, it is observed that the TLC model requires less CPU time than the Kachanov-Rabotnov model. It is also observed that the strain rate sensitivity of the Kachanov-Rabotnov model is not a factor for the TLC model. The greatest influence on the CPU time required for the TLC model is the relative time-shift percentage. Figures 5.1 and 5.2 illustrate these relationships.

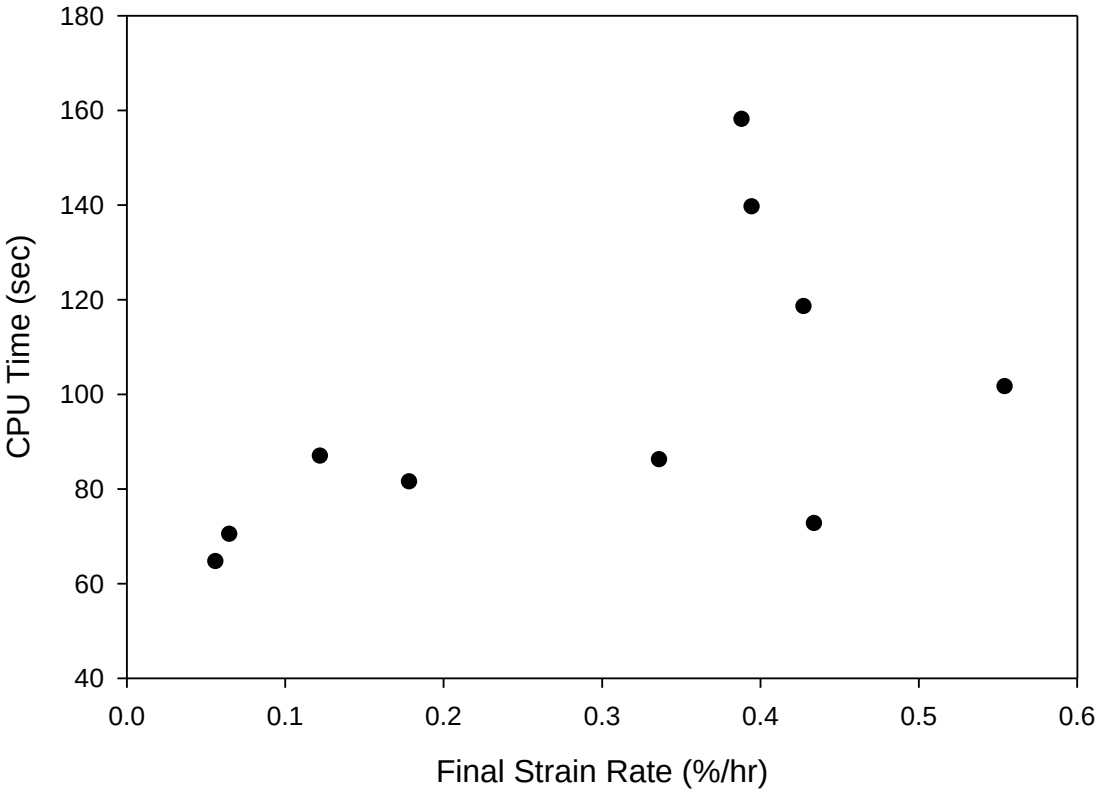

Figure 5.1: Illustration of slight strain rate sensitivity of Kachanov-Rabotnov model

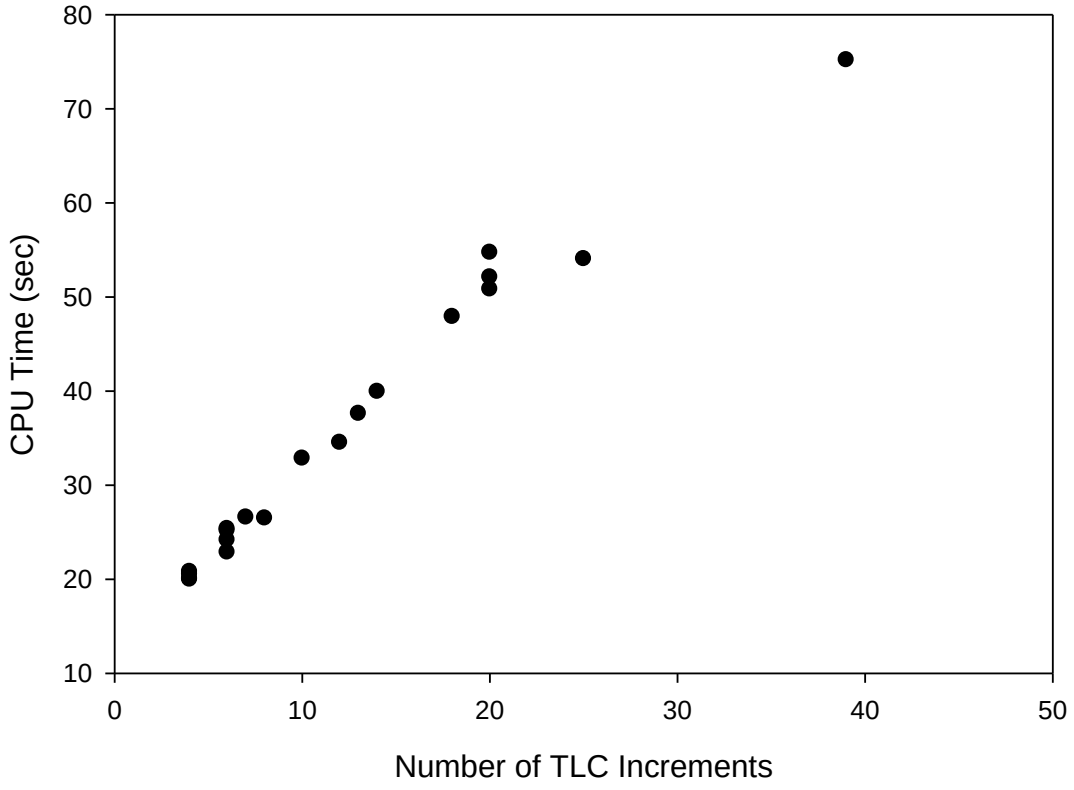

Figure 5.2: Illustration of linear relationship between CPU Time and # of TLC increments

CHAPTER 6: CONCLUSION

The goal of this research is to develop a reduced-order constitutive model that would require reduced CPU time to simulate compared to the Kachanov-Rabotnov tertiary creep model while still maintaining a satisfactory degree of accuracy. By utilizing a novel mathematical manipulation, a model comprised of a variable number of secondary creep curves, which are easy for finite element packages to solve, was developed that allows for tertiary creep to be simulated more efficiently, even until rupture. Tertiary creep models are susceptible to strain rate sensitivity because of the Newton-Raphson mechanics that are used in non-linear systems to converge upon a solution. The TLC model is free of strain rate sensitivity because of its multi-linear nature. It is observed that when attempting to minimize error by utilizing a very small time-shift, that solve times can potentially exceed that of the Kachanov-Rabotnov model. As the number of TLC increments decreases, the amount of error increases and the CPU time required decreases. In some cases smaller increment TLC models were more accurate in predicting final strain rates than higher increment TLC models or the Kachanov-Rabotnov model, but this is entirely dependent on the material constants and experimental parameters used. In general, the TLC model solves faster than the Kachanov-Rabotnov model and is very similar in overall correlation to physical data per the cumulative strain energy approximation. The TLC model captures the near-rupture portion of tertiary creep more accurately than the Kachanov-Rabotnov model as well. The TLC model does not solve as fast as the Norton secondary creep model, but it characterizes the creep at a level that exceeds the increase in CPU time.

CHAPTER 7: FUTURE WORK

The TLC model is governed by Kachanov-Rabotnov material constants that portray both stress and temperature-dependence. To further increase the robustness of the reduced-order constitutive model, it would be necessary to incorporate stress and temperature mathematical relationships into a UPF that would be linked to the ANSYS environment. This would allow more complex geometries that experience stress and temperature gradients to be simulated. In more complex geometries, the applied stress evolves as the strain increases and this would affect the stress-dependent constants. In its current state, the TLC model is only applicable to single element simulations. If a complex geometry could be simulated with the TLC model, it would reveal the true value of the TLC model. It is hypothesized that the margin of required CPU time between the TLC model and tertiary creep models will grow as component complexity increases, so future testing to prove or disprove this is necessary.

Redesigning the method for determining the appropriate values of n that result in the TLC generated lines is also necessary so that stepped isostress and stepped isotemperature simulations can be carried out. In its current state, it is not possible to simulate such experiments because the TLC generated lines are based on tangent and chord points that satisfy the numerical conditions without regards to stress or temperature. The entire numerical routine will have to be redesigned to accomplish this.

APPENDIX: SOURCE CODES

APPENDIX 1: MATLAB TLC MODEL MAIN ROUTINE

```
clc;
closeall;
clearall;
%define stress (MPa)
temp = input('Enter Stress (ksi): ');
stressksi = temp;
stress=stressksi/.1450377;
%define temperature (F)
temp = input('Enter Temperature (F): ');
temperature = temp;
%define the end time (hrs)
temp = input('Enter Final Time (hr): ');
tfinal = temp;
%tfinal=1300;
tfinali=int32(tfinal);
%Define TimeShift (hrs)
temp = input('Enter TimeShift: ');
timeshift = temp;
%Define data type
t1=0:1:tfinal;
%Define the four constants that define the Kachanov-Rabotnov Strain Equation:
%       strain = (A*stress^-chi)/(M*(-1+n-phi))*(-1*stress^n+(1-
M*stress^chi*time*(1+phi))*(stress*(1-M*stress^chi*time*(1+phi))^(-
1/(1+phi)))^n)
%temp = input('Enter "A": ');
%A = temp;
%temp = input('Enter "n": ');
%n = temp;
%temp = input('Enter "M": ');
%M = temp;
%temp = input('Enter "chi": ');
%chi = temp;
%temp = input('Enter "phi": ');
%phi = temp;
fori=2:tfinal+1
y1(i)=0;
%y1(i)=(A*stress^-chi)/(M*(-1+n-phi))*(-1*stress^n+(1-
M*stress^chi*t1(i)*(1+phi))*(stress*(1-M*stress^chi*t1(i)*(1+phi))^(-
1/(1+phi)))^n);
y1rate(i)=A*(stress/(1-(phi+1)*M*stress^chi*t1(i))^(1/(phi+1)))^n;
y1(i)=y1(i-1)+y1rate(i);
t2(i)=t1(i)+timeshift;
y2(i)=y1(i);
end
figure;
plot(t1,y1,t2,y2);
holdon
%setting up slope and determining average slope for first section
%the idivide will change depending on the number of points
p=idivide(tfinali,8);
%m is the nth data point where primary creep ends, done manually
```

```
%taking the average slope of the first chunk of points eliminates outliers
%that are present in almost all physical data
m=1;
fori=0:p-m
slope(i+1)=(y1(i+m+1)-y1(i+m))/(t1(i+m+1)-t1(i+m));
end
meanslope=mean(slope);
k=1;
intercepts(k,1)=0;
intercepts(k,2)=0;
intercepts(k,3)=0;
k=k+1;
[i,XX2,YY2]=bluetogreen(tfinal,meanslope,t1,y1,t2,y2);
if XX2==0
disp('timeshift too large, intersection not found')
end
intercepts(k,1)=i;
intercepts(k,2)=XX2;
intercepts(k,3)=YY2;
k=k+1;
flag=2;
while flag==2
[XX1,YY1,XX2,YY2,flag,ii,j,meanslope]=greentoblue(tfinal,meanslope,t1,y1,t2,y
2,XX2,YY2,i);
if flag==1
intercepts(k,1)=ii;
intercepts(k,2)=XX1;
intercepts(k,3)=YY1;
        k=k+1;
end
if flag==2
intercepts(k,1)=ii;
intercepts(k,2)=XX1;
intercepts(k,3)=YY1;
        k=k+1;
intercepts(k,1)=j;
intercepts(k,2)=XX2;
intercepts(k,3)=YY2;
        k=k+1;
i=j;
end
end
plot(intercepts(:,2),intercepts(:,3), 'black');
xlabel('time, t (hr)');
ylabel('strain (mm/mm)');
holdon
%Error Calculation (%)
SimulatedRunTime=intercepts(k-1,2);
ActualRunTime=tfinal;
%Here we assume a value for either A or n so that we can solve for the
%other, this is an easy method to find these parameters without resorting
%to complex regression routines
%for i=2:k-1
%    AA(i-1)=intercepts(i,3)/(intercepts(i,2)*stress^n);
```

```
%    nn(i-1)=log(intercepts(i,3)/(A*intercepts(i,2)))/(log(stress));
%    SStrain1(i)=AA(i-1)*stress^n*intercepts(i,2);
%    SStrain2(i)=A*stress^nn(i-1)*intercepts(i,2);
%end
fori=1:k-2
    Nslope(i)=(intercepts(i+1,3)-intercepts(i,3))/((intercepts(i+1,2)-
intercepts(i,2)));
NNN(i)=(log(Nslope(i)/A))/(log(stress));
yintercept(i)=intercepts(i+1,3)-Nslope(i)*intercepts(i+1,2);
end
%Either choose the constant A and use the nn array or choose the constant n
%and use the AA array values for simulating
%figure
%plot(intercepts(:,2),intercepts(:,3), 'black')
%hold on
%plot(intercepts(:,2),SStrain1, 'red');
%plot(intercepts(:,2),SStrain2, 'blue');
eq=numel(NNN)
fid = fopen('C:\OPT\constants.txt','wt');
fprintf(fid,'%f\n',NNN);
fclose(fid);
fid = fopen('C:\OPT\intercepts.txt','wt');
fprintf(fid,'%f\n',yintercept);
fclose(fid);
fid = fopen('C:\OPT\times.txt','wt');
fprintf(fid,'%f\n',intercepts(:,2));
fid = fopen('C:\OPT\parameters.txt','wt');
fprintf(fid,'%e\n',A,stress,temperature,tfinal,eq);
fclose(fid);
RunTimeErrorPercent=((ActualRunTime-SimulatedRunTime)/(ActualRunTime))*100
StrainErrorPercent=((y1(1,tfinal+1)-intercepts(eq+1,3))/(y1(1,tfinal+1)))*100
```

APPENDIX 2: MATLAB TLC MODEL BLUETOGREEN FUNCTION

This MATLAB function is called in the main program to generate the initial projected line from the original creep curve to the time-shifted creep curve.

```
function [i,XX2,YY2] = bluetogreen (tfinal,meanslope,t1,y1,t2,y2)
XX2=0;
YY2=0;
fori=2:(tfinal)-1
ifmeanslope*t2(i)<=y2(i)-0.000000005;
                YY2=(y2(i)+y2(i-1))/2;
                XX2=((t2(i)+t2(i-1))/2);
break
end
end
```

APPENDIX 3: MATLAB TLC MODEL GREENTOBLUE FUNCTION

This MATLAB function is called in the main program to generate each successive projected line from the time-shifted creep curve to the original creep curve.

```
function [XX1,YY1,XX2,YY2,flag,ii,j,meanslope] = greentoblue
(tfinal,meanslope,t1,y1,t2,y2,XX2,YY2,i)
flag=0;
ii=i;
XX1=0;
YY1=0;
j=0;
while ii<=(tfinal)-1 && flag==0
ifmeanslope*(t1(ii)-XX2)+YY2>=y1(ii)-0.000000005;
       YY1=(y1(ii)+y1(ii-1))/2;
       XX1=((t1(ii)+t1(ii-1))/2);
flag=1;
       j=ii;
while j<=(tfinal-1) && flag==1
ifmeanslope*(t2(j)-XX1)+YY1<=y2(j)-0.000000005;
            YY2=(y2(j)+y2(j-1))/2;
            XX2=((t2(j)+t2(j-1))/2);
flag=2;
end
            j=j+1;
end
end
ii=ii+1;
%this resets the i and increases the slope if an intercept was not
%found
if ii==tfinal;
meanslope=1.00005*meanslope;
ii=i;
ifmeanslope>=1
flag=3;
end
end
end
```

APPENDIX 4: ANSYS INPUT FILE (TLC Model)

```
finish
/clear
! ANSYS command file to perform creep
! on a differential element within a Dogbone Specimen
/title, Creep Deformation and Rupture Using TLC Method
/OUTPUT,C:\OPT\prep,txt,,   ! Send output to file
/CONFIG,NRES,1000000
!
/PREP7                              ! Enter preprecessing phase
!
! Parameter Declaration
!
!
! Enter in the number of linear equations that MATLAB generated below
*DIM,parameters,,5
*VREAD, parameters(1), C:\OPT\parameters,txt
(E13.5)
eq=parameters(5)
eqtwo=eq+1
*DIM,constants,,eq
*VREAD, constants(1), C:\OPT\Constants,txt
(E13.5)
*DIM,times,,eqtwo
*VREAD, times(1), C:\OPT\times,txt
(E13.5)
! Thermal/Mechanical Conditions
!
temp_F = parameters(3)              ! in deg F
load_step_time=times(eqtwo)         ! in hr
stress = parameters(2)              ! in MPa
stress_ksi = stress*0.1450377       ! in ksi
temp_C = 5.0/9.0*(temp_F-32.0)      ! in deg C
temp_K = temp_C+273.15              ! in K
temp_ref = 0.0                      ! Reference temperature in K
!
! Geometric: [mm]
DIM_Neck=0.25*25.4/2
DIM_GRIP=0.50*25.4/2
DIM_L=4*25.4
DIM_R=1*25.4
DIM_A=0.5*25.4
DIM_B=(0.5+0.484)*25.4
!
! History Options
!
!load_init_time=0.0001                ! in hr
!load_mini_time=0.00001                ! in hr
!load_maxi_time=100                   ! in hr
load_ramp_time=1                     ! in hr
!
! Material Properties
```

```
!
A_nort=parameters(1)
n_nort=constants(1)              ! Temperature independent secondary creep
coefficent
report=1.0
!
! Job Options
!
data_freq = 10                   ! frequency of data writing
!
!*********************************************************************
***
pi=4*atan(1)
pressure=stress*pi*DIM_Neck**2/(pi*DIM_GRIP**2)
!*********************************************************************
***
!
! Specimen Geometry:
!
! Keypoints
k,  1,   0.0,    0.0,    ,0.0
k,  2,   0.0,    DIM_A    ,0.0
k,  3,   0.0,    DIM_L/2    ,0.0
k,  4,   DIM_GRIP,     DIM_L/2    ,0.0
k,  5,   DIM_GRIP,     DIM_B    ,0.0
k,  6,   DIM_Neck,     DIM_A    ,0.0
k,  7,   DIM_Neck,     0.0    ,0.0
!
!
!
! Lines
L,  1,  7         ! Line 1
L,  1,  2         ! Line 2
L,  2,  3         ! Line 3
L,  3,  4         ! Line 4
L,  4,  5         ! Line 5
L,  6,  7         ! Line 6
L,  2,  6         ! Line 7
LARC,6,5,7,DIM_R,
!
! Area
FLST,2,4,4
FITEM,2,1
FITEM,2,6
FITEM,2,2
FITEM,2,7
AL,P51X
FLST,2,5,4
FITEM,2,8
FITEM,2,5
FITEM,2,3
FITEM,2,4
FITEM,2,7
AL,P51X
```

```
AGLUE,all

!*************************************************************************
***

!*************************************************************************
***
! Element Type: Sweep 2D Area
ET,1,PLANE183,,,1

! Create 2D Mesh
type,1
AESIZE,1,0.2
AMESH, 1
AESIZE,2,0.5
AMESH, 2
!*************************************************************************
***
!
! Define Properties of Material 1 (for built-in norton secondary creep no
UPF)
!
MP, EX, 1, e_mod                  ! in MPa
MP, DENS, 1, mass_dens            ! in g/mm3
MP,NUXY,1,0.33
TB,CREEP,1,1,,10                 ! Activate NORTON creep
TBTEMP, temp_ref
TBDATA,1,A_nort,n_nort            ! Material Constants
!
! Boundary Conditions and Loads:
DL,       2, ,SYMM
DL,       3, ,SYMM
DL,1,,UY,0.0
SFL,4,PRES,-Pressure

! Temperature boundary conditions
!
TUNIF, temp_C
TREF, temp_ref
TOFFST, 0.
!
! Solution Option
OUTPR,ALL
! USRCAL,Usolfin
!
FINISH                          ! Finish pre-processing
!
/SOLU                           ! Begin Solution phase
!
! Step 1 - Ramp Mechanical Load
!
NCNV, 0, 1e60,,,
antype,0                        ! static analysis
```

```
nropt,auto                      ! Newton Raphson = auto
lnsrch,auto                     ! Line search on
NLGEOM,OFF                      ! Non-linear geometry
SOLCONTROL,ON                   ! Solution control - optimized nonlinear
TIME, load_ramp_time            ! in hours
DELTIM, 0.0001, 0.00001, 100
AUTOTS,ON                       ! AUTOMATIC TIME STEPPING
CRPLIM,10.0,1                   ! Creep ration limit of 2 applied for implicit
creep
OUTRES,ESOL,ALL                 ! store element RESULTS
RATE,OFF
KBC,0
SOLVE                           ! Solve for step 1
!
! Step 2 - Keep Mechanical Load Constant
!
NCNV, 0, 1e60,,,
antype,0                        ! static analysis
nropt,auto                      ! Newton Raphson = auto
lnsrch,auto                     ! Line search on
NLGEOM,OFF                      ! Non-linear geometry
SOLCONTROL,ON                   ! Solution control - optimized nonlinear
TIME, times(2)                  ! in hours
DELTIM, times(2)
AUTOTS,OFF                      ! AUTOMATIC TIME STEPPING
OUTRES,ESOL,ALL                 ! store element RESULTS
CRPLIM,10.0,1
RATE,ON
KBC,1
SAVE
SOLVE                           ! Solve for step 2
!
! Steps 3 Onwards
!
*DO,i,2,eq
n_nort=constants(i)
timerange=times(i+1)
timechange=timerange/4
TB,CREEP,1,1,,10
TBTEMP, temp_ref
TBDATA,1,A_nort,n_nort          ! Material Constants
TIME, timerange                 ! in hours
DELTIM, timerange-times(i)
AUTOTS,OFF
OUTRES,ESOL,ALL                 ! store element RESULTS
RATE,ON
KBC,1
SAVE
SOLVE                           ! Solve for subsequent steps
*ENDDO
SAVE
FINISH
!
/POST26
```

```
/OUTPUT,C:\OPT\results,txt,,
ESOL,4,16,2,S,y,Sy              ! Stress
ESOL,5,16,2,EPEL,Y,EY           ! Store the elastic strain
ESOL,6,16,2,EPCR,Y,ECRY         ! Store the creep strain
PRVAR,4,5,6                     ! PRINT VARIABLES VS. TIME
FINISH
```

APPENDIX 5: ANSYS INPUT FILE (NORTON MODEL)

```
finish
/clear
! ANSYS command file to perform creep
! on a differential element within a bone specimen.
! written by D.L. May (1-21-14)
!
/title, Creep Deformation and Rupture Using TLC Method
/OUTPUT,C:\OPT\prep,txt,,   ! Send output to file
/CONFIG,NRES,1000000
!
/PREP7                              ! Enter preprecessing phase
!
! Parameter Declaration
!
! These parameters are not required; i.e. one could
! directly enter in the coordinates into the keypoint
! definition below. However, using parameters makes it very easy to
! quickly make changes to this model!
!
!
temp_F = 1400             ! in deg F
load_step_time=975        ! in hr
stress = 148          ! in MPa
stress_ksi = stress*0.1450377      ! in ksi
temp_C = 5.0/9.0*(temp_F-32.0)     ! in deg C
temp_K = temp_C+273.15             ! in K
temp_ref = 0.0                     ! Reference temperature in K
!
! Geometric: [mm]
DIM_Neck=0.25*25.4/2
DIM_GRIP=0.50*25.4/2
DIM_L=4*25.4
DIM_R=1*25.4
DIM_A=0.5*25.4
DIM_B=(0.5+0.484)*25.4
!
! History Options
!
load_init_time=0.0001               ! in hr
load_mini_time=0.00001               ! in hr
load_maxi_time=100                  ! in hr
load_ramp_time=1                    ! in hr
!
! Material Properties
!
A_nort=2.25E-32
n_nort=12.4            ! Temperature independent secondary creep coefficent
report=1.0
!
! Job Options
!
```

```
data_freq = 10                    ! frequency of data writing
!
!*****************************************************************************
***
pi=4*atan(1)
pressure=stress*pi*DIM_Neck**2/(pi*DIM_GRIP**2)
!*****************************************************************************
***
!
! Specimen Geometry:
!
! Keypoints
k,  1,   0.0,    0.0,    ,0.0
k,  2,   0.0,    DIM_A    ,0.0
k,  3,   0.0,    DIM_L/2    ,0.0
k,  4,   DIM_GRIP,     DIM_L/2    ,0.0
k,  5,   DIM_GRIP,     DIM_B    ,0.0
k,  6,   DIM_Neck,     DIM_A    ,0.0
k,  7,   DIM_Neck,     0.0    ,0.0
!
!
!
! Lines
L,  1,  7          ! Line 1
L,  1,  2          ! Line 2
L,  2,  3          ! Line 3
L,  3,  4          ! Line 4
L,  4,  5          ! Line 5
L,  6,  7          ! Line 6
L,  2,  6          ! Line 7
LARC,6,5,7,DIM_R,
!
! Area
FLST,2,4,4
FITEM,2,1
FITEM,2,6
FITEM,2,2
FITEM,2,7
AL,P51X
FLST,2,5,4
FITEM,2,8
FITEM,2,5
FITEM,2,3
FITEM,2,4
FITEM,2,7
AL,P51X

AGLUE,all

!*****************************************************************************
***

!*****************************************************************************
***
```

```
! Element Type: Sweep 2D Area
ET,1,PLANE183,,,1

! Create 2D Mesh
type,1
AESIZE,1,0.2
AMESH, 1
AESIZE,2,0.5
AMESH, 2
!*************************************************************************
***
!
! Define Properties of Material 1 (for built-in norton secondary creep no
UPF)
!
MP, EX, 1, e_mod                  ! in MPa
MP, DENS, 1, mass_dens            ! in g/mm3
MP,NUXY,1,0.33
TB,CREEP,1,1,,10                  ! Activate NORTON creep
TBTEMP, temp_ref
TBDATA,1,A_nort,n_nort            ! Material Constants
!
! Boundary Conditions and Loads:
DL,       2, ,SYMM
DL,       3, ,SYMM
DL,1,,UY,0.0
SFL,4,PRES,-Pressure

! Temperature boundary conditions
!
TUNIF, temp_C
TREF, temp_ref
TOFFST, 0.
!
! Solution Option
OUTPR,ALL
! USRCAL,Usolfin
!
FINISH                          ! Finish pre-processing
!
/SOLU                           ! Begin Solution phase
!
! Step 1 - Ramp Mechanical Load
!
NCNV, 0, 1e60,,,
antype,0                        ! static analysis
nropt,auto                      ! Newton Raphson = auto
lnsrch,auto                     ! Line search on
NLGEOM,OFF                      ! Non-linear geometry
SOLCONTROL,ON                   ! Solution control - optimized nonlinear
TIME, load_ramp_time            ! in hours
DELTIM, load_init_time, load_mini_time, load_maxi_time
AUTOTS,ON                       ! AUTOMATIC TIME STEPPING
```

```
CRPLIM,10.0,1                  ! Creep ration limit of 2 applied for implicit
creep
OUTRES,ESOL,ALL                ! store element RESULTS
RATE,OFF
KBC,0
SOLVE                          ! Solve for step 1
!
! Step 2 - Keep Mechanical Load Constant
!
NCNV, 0, 1e60,,,
antype,0                       ! static analysis
nropt,auto                     ! Newton Raphson = auto
lnsrch,auto                    ! Line search on
NLGEOM,OFF                     ! Non-linear geometry
SOLCONTROL,ON                  ! Solution control - optimized nonlinear
TIME, load_step_time           ! in hours
DELTIM, load_step_time
AUTOTS,OFF                     ! AUTOMATIC TIME STEPPING
OUTRES,ESOL,ALL                ! store element RESULTS
CRPLIM,10.0,1                  ! Creep ration limit of 2 applied for implicit
creep
RATE,ON
KBC,1
SAVE
SOLVE                          ! Solve for step 2
FINISH
!
/POST26
/OUTPUT,C:\OPT\results,txt,,
ESOL,4,16,2,S,y,Sy              ! Stress
ESOL,5,16,2,EPEL,Y,EY           ! Store the elastic strain
ESOL,6,16,2,EPCR,Y,ECRY         ! Store the creep strain
PRVAR,4,5,6                     ! PRINT VARIABLES VS. TIME
FINISH
```

APPENDIX 6: ANSYS INPUT FILE (KACHANOV-RABOTNOV MODEL)

```
finish
/clear
! ANSYS command file to perform creep
! on a differential element within a dog bone specimen.
! written by D.L. May (1-21-14)
!
/title, Creep Deformation and Rupture Using TLC Method
/OUTPUT,C:\OPT\prep,txt,,   ! Send output to file
/CONFIG,NRES,1000000
!
/PREP7                              ! Enter preprecessing phase
!
! Parameter Declaration
! Thermal/Mechanical Conditions
!
stress_ksi = 24          ! in ksi
stress = stress_ksi/0.1450377      ! in MPa
temp_C = 760     ! in deg C
temp_K = temp_C+273.15             ! in K
temp_ref = 0.0                     ! Reference temperature in K
!
! Geometric: [mm]
DIM_Neck=0.25*25.4/2
DIM_GRIP=0.50*25.4/2
DIM_L=4*25.4
DIM_R=1*25.4
DIM_A=0.5*25.4
DIM_B=(0.5+0.484)*25.4
!
! History Options
!
load_step_time=1000       ! in hr
load_init_time=0.0001                ! in hr
load_mini_time=0.00001               ! in hr
load_maxi_time=100                  ! in hr
load_ramp_time=1                    ! in hr
!
! Material Properties
!
A_nort=2.25E-32
n_nort=12.4
M_kr=5.5E-11
chi_kr=3
phi_kr=3
report=1.0
!
! Job Options
!
data_freq = 10                   ! frequency of data writing
omeg_init=0.                       ! initial damage state
omeg_dot_init=0.                   ! initial damage rate
```

```
crepeqv=0.                          ! initial equivalent creep strain
!
!*****************************************************************************
***
pi=4*atan(1)
pressure=stress*pi*DIM_Neck**2/(pi*DIM_GRIP**2)
!*****************************************************************************
***
!
! Specimen Geometry:
!
! Keypoints
k,  1,   0.0,    0.0,    ,0.0
k,  2,   0.0,    DIM_A    ,0.0
k,  3,   0.0,    DIM_L/2    ,0.0
k,  4,   DIM_GRIP,     DIM_L/2    ,0.0
k,  5,   DIM_GRIP,     DIM_B    ,0.0
k,  6,   DIM_Neck,     DIM_A    ,0.0
k,  7,   DIM_Neck,     0.0    ,0.0
!
!
!
! Lines
L,  1,  7          ! Line 1
L,  1,  2          ! Line 2
L,  2,  3          ! Line 3
L,  3,  4          ! Line 4
L,  4,  5          ! Line 5
L,  6,  7          ! Line 6
L,  2,  6          ! Line 7
LARC,6,5,7,DIM_R,
!
! Area
FLST,2,4,4
FITEM,2,1
FITEM,2,6
FITEM,2,2
FITEM,2,7
AL,P51X
FLST,2,5,4
FITEM,2,8
FITEM,2,5
FITEM,2,3
FITEM,2,4
FITEM,2,7
AL,P51X

AGLUE,all

!*****************************************************************************
***

!*****************************************************************************
***
```

```
! Element Type: Sweep 2D Area
ET,1,PLANE183,,,1

! Create 2D Mesh
type,1
AESIZE,1,0.2
AMESH, 1
AESIZE,2,0.5
AMESH, 2
!*************************************************************************
***
!
! Define Properties of Material 1
!
MP, EX, 1, e_mod                 ! in MPa
MP, DENS, 1, mass_dens           ! in g/mm3
MP,NUXY,1,0.33
TB,CREEP,1,1,,100                ! Activate USERCREEP
TBTEMP, temp_ref
TBDATA,1,A_nort,n_nort,M_kr,chi_kr,phi_kr          ! Material Constants
TB,STATE,1,,3
TBDATA,1,omeg_init,omeg_dot_init,crepeqv  ! Initialize the 3 state variables.
!
! Temperature boundary conditions
!
TUNIF, temp_C
TREF, temp_ref
TOFFST, 0.
!
! Boundary Conditions and Loads:
DL,       2, ,SYMM
DL,       3, ,SYMM
DL,1,,UY,0.0
SFL,4,PRES,-Pressure
!
! Solution Option
OUTPR,ALL,LAST
! USRCAL,Usolfin
!
FINISH                          ! Finish pre-processing
!
/SOLU                           ! Begin Solution phase
! Step 1 - Ramp Mechanical Load
NCNV, 0, 1e60,,,
antype,0                        ! static analysis
nropt,auto              ! Newton Raphson = auto
lnsrch,auto             ! Line search on
NLGEOM,OFF                      ! Non-linear geometry
SOLCONTROL,ON                   ! Solution control - optimized nonlinear
TIME, load_ramp_time            ! in seconds
DELTIME, load_init_time, load_mini_time, load_maxi_time
AUTOTS,ON                       ! AUTOMATIC TIME STEPPING
CRPLIM,0,1                      ! Creep ration limit of 2 applied for implicit
creep
```

```
OUTRES,ESOL,ALL                ! store element RESULTS
OUTRES,SVAR,ALL
RATE,OFF
KBC,1
SOLVE                          ! Solve for step 1
!
!
! Step 2 and so on - Keep Mechanical Load Constant
!
antype,0                       ! static analysis
nropt,auto                       ! Newton Raphson = auto
lnsrch,auto                    ! Line search on
NLGEOM,OFF                     ! Non-linear geometry
SOLCONTROL,ON                  ! Solution control - optimized nonlinear
TIME, load_step_time           ! in hrs
DELTIME, load_init_time, load_mini_time, load_maxi_time
AUTOTS,ON                      ! AUTOMATIC TIME STEPPING
OUTRES,ESOL,ALL                ! store element RESULTS
OUTRES,SVAR,ALL                ! store element RESULTS
CRPLIM,10.0,1                  ! Creep ration limit of 2 applied for implicit
creep
RATE,ON
KBC,1
SOLVE                          ! Solve for step 2 and so on
FINISH
!
/POST26
 NUMVAR,200
/OUTPUT,C:\OPT\results,txt,,
ESOL,4,16,2,S,y,Sy              ! Stress
ESOL,5,16,2,EPEL,Y,EY           ! Store the elastic strain
ESOL,6,16,2,EPCR,Y,ECRY         ! Store the creep strain
ESOL,7,16,2,SVAR,1,Damage       ! Stores Damage in X for node 6
ESOL,8,16,2,SVAR,2,Rate         ! Stores Damage in X for node 6
PRVAR,4,5,6,7,8                 ! PRINT VARIABLES VS. TIME
FINISH
```

REFERENCES

[1] Technology Characterization: Gas Turbines". Energy and Environmental Analysis, Arlington, VA, 2008.

[2] Y.S. Na and J.H. Lee, "Interpretation of viscous deformation of bulk metallic glasses based on the nabarro-herring creep model," *Journal of Materials Processing Technology*, Vol. 187-188, pp. 786-790, 2007.

[3] S.M. Haghighat, G. Eggeler, and D. Raabe, "Effect of climb on dislocation mechanisms and creep rates in γ-strengthened Ni base superalloy single crystals: a discrete dislocation dynamics study," *Acta Materialia*, Vol. 61, pp. 3709-3723, 2013.

[4] J. Betten, "Constitutive Models of Creep," in *Creep Mechanics*, 3rd ed. Berlin, Germany: Springer, 2008, pp. 17-84.

[5] T.M Pollock and S. Tin, "Nickel-based superalloys for advanced turbine engines: chemistry, microstructure, and properties," *Journal of Propulsion and Power*, Vol. 22, pp. 361-374, 2006.

[6] D.L. May, A.P. Gordon, and D.S. Segletes, "The application of the norton-bailey law for creep prediction through power law regression," presented at the ASME Turbo Expo: Turbine Technical Conference and Exposition, San Antonio, Texas, 2013.

[7] F.H. Norton, *The Creep of Steel at High Temperatures*, London, U.K.: McGraw-Hill, 1929.

[8]Evans, R., Parker, J., Wilshire, B. "The Theta Projection Concept – A Model-based Approach to Design and LifeExtension of Engineering Plant," *International Journal of Pressure Vessels and Piping*, Vol. 50, Issues 1-3, pp. 147-160, 1992.

[9] L.M. Kachanov, *The Theory of Creep*, Boston Spa, U.K.: Kennedy, 1967.

[10] Y.N. Rabotnov, *Creep Problems in Structural Members*, North-Holland, Netherlands, 1969.

[11] Y. Kariya, M. Otsuka, and W.J. Plumbridge, "The Constitutive Creep Equation for a Eutectic Sn-Ag Alloy Using the Modified Theta-Projection Concept," *Journal of Electronic Materials*, Vol. 32, No. 12, 2003.

[12] C. Stewart and A. Gordon, "Modeling the Temperature Dependence of Tertiary Creep Damage of a Ni-Based Alloy," *Journal of Pressure Vessel Technology*, Vol. 131, 2009.

[13] M.C. Araújo, "Non-Linear Kinematic Hardening Model for Multiaxial Cyclic Plasticity," M.S. thesis, Louisiana State University, Baton Rouge, 2002.

[14] E. Gal and J. Fish, "Anisotropic Micromechanical Creep Damage Model for Composite Materials: A Reduced-Order Approach," *International Journal for Multiscale Computational Engineering*, Vol. 6, No. 2, 2008.

[15] E. Bellenger and P. Bussy, "Phenomenological Modeling and Numerical Simulation of Different Modes of Creep Damage Evolution," *International Journal of Solids and Structures*, Vol. 38, pp. 578-604, 2001.

[16] C. Stewart, "Tertiary creep damage modeling of a transversely isotropic ni-based superalloy," M.S. thesis, University of Central Florida, Orlando, 2009.

[17] D. Day and A. Gordon, "A modified theta projection creep model for a nickel-based super-alloy," presented at the ASME Turbo Expo: Turbine Technical Conference and Exposition, San Antonio, Texas, 2013.

[18] R. Lim, M. Sauzay, F. Dalle, I. Tournie, P. Bonnaillie, and A.F. Gourgues-Lorenzon, "Modelling and Experimental Study of the Tertiary Creep Stage of Grade 91 Steel," *International Journal of Fracture Mechanics*, Vol. 169, pp. 213-228, 2011.

[19] E.W. Hart, "Theory of the Tensile Test," *Acta Metallurgica*, Vol. 15, No. 2, Feb., pp. 161-445, 1967.

[20] J.F. Wen, S.T. Tu, X.L. Gao, andJ.N. Reddy, "Simulations of creep crack growth in 316 stainless steel using a novel creep-damage model," *Journal of Engineering Fracture Mechanics*, Vol. 98, pp. 169-184, 2013.

[21] B. Zhao, X.S. Wang, and Z. Feng, "Experiment and simulation of creep damage for duralumin alloy 2A12," *Journal of Materials Science and Engineering*, Vol. 513-514, pp. 91-96, 2009.

[22] D. Alonso, J.M. Vega, A. Velazquez, and V. Pablo, "Reduced-Order Modeling of Three-Dimensional External Aerodynamic Flows," *Journal of Aerospace Engineering*, Vol. 25, No. 4, pp. 588-599, 2012.

[23] A. LaBryer, P.J. Attar, and P. Vedula, "Optimal Spatiotemporal Reduced Order Modeling, Part II: Application to a Nonlinear Beam," *Journal of Computational Mechanics*, Vol. 52, pp. 433-451, 2013.

[24] S. Tian, Z. Zeng, L. Fushun, C. Zhang, and C. Liu, "Creep behavior of a 4.5%-Re single crystal nickel-based superalloy at intermediate temperatures," *Journal of Materials Science and Engineering*, Vol. 543, pp. 104-109, 2012.

[25] Y. Xingfu, T. Sugui, W. Minggang, Z. Shu, L. Xudong, and C. Shusen, "Creep behaviors and effect factors of single crystal nickel-based superalloys," *Journal of Materials Science and Engineering*, Vol. 499, pp. 352-359, 2009.